



DOCUMENT 256-93

JOINT RANGE INSTRUMENTATION
ACCURACY IMPROVEMENT GROUP
AND
ELECTRONIC TRAJECTORY
MEASUREMENTS GROUP

IRIG RADAR CALIBRATION CATALOG

The IRIG Error Model Reference for Radar Calibrations Version 2

WHITE SANDS MISSILE RANGE
KWAJALEIN MISSILE RANGE
YUMA PROVING GROUND
DUGWAY PROVING GROUND
ELECTRONIC PROVING GROUND

ATLANTIC FLEET WEAPONS TRAINING FACILITY
NAVAL AIR WARFARE CENTER WEAPONS DIVISION
NAVAL AIR WARFARE CENTER AIRCRAFT DIVISION
NAVAL UNDERSEA WARFARE CENTER DIVISION NEWPORT

30TH SPACE WING
45TH SPACE WING
AIR FORCE FLIGHT TEST CENTER
AIR FORCE DEVELOPMENT TEST CENTER
AIR FORCE WEAPONS AND TACTICS CENTER
DETACHMENT 2, SPACE AND MISSILE SYSTEMS CENTER

**DISTRIBUTION A: APPROVED FOR PUBLIC RELEASE;
DISTRIBUTION IS UNLIMITED**

DOCUMENT 256-93

IRIG RADAR CALIBRATION CATALOG

**The IRIG Error Model Reference for Radar Calibrations
Version 2**

OCTOBER 1993

Prepared by

**JOINT RANGE INSTRUMENTATION ACCURACY IMPROVEMENT GROUP
AND
ELECTRONIC TRAJECTORY MEASUREMENTS GROUP
RANGE COMMANDERS COUNCIL**

Published by

**Secretariat
Range Commanders Council
U.S. Army White Sands Missile Range,
New Mexico 88002-5110**

PREFACE

The Range Commanders Council (RCC) was originated to preserve and enhance the efficiency, effectiveness, and economical operation of member ranges, individually and collectively, thereby increasing the national capability for research, development, and operational testing and evaluation.¹ In the area of RADio Detection And Ranging (RADAR), two standing groups of the RCC have had a common interest. The two groups are the Electronic Trajectory and Measurement Group (ETMG) and the Joint Range Instrumentation Accuracy Improvement Group (JRIAIG). The common interest in radar systems has been the overall accuracy of such instruments. Presently, radar systems are used for tracking a wide variety of targets ranging from submunitions and unmanned vehicles to aircraft, missiles, and satellites. In each of these tracking situations, the accuracy of the final results is of primary importance.

The raw range, azimuth, elevation, and range-rate data from radar systems contain both systematic and random errors. Random errors are typically estimated using statistical methods and may be minimized by the use of optimal filter/smoothing techniques. Systematic errors, on the other hand, require calibration (via satellite tracking or similar means), mathematical modeling, and mechanical alignment to remove or reduce their effects. The measurement and control of these errors can be very difficult and time consuming.

The earlier version of this document IRIG document 256-77 (formerly 135-77), addressed a limited number of error terms with an additional section on refraction. Ranges which had calibration procedures for these terms were identified along with their procedures for assessment and measurement. This document has remained virtually untouched since its first publication in 1977. Since that time, other ranges have adopted rigorous radar calibration procedures, enlarged the number of error terms, and initiated regular performance monitoring of their radar systems. The JRIAIG tasked the Air Force Flight Test Center to revise the original document and to expand on its foundation by identifying specific error models and procedures which will serve as generic starting points for future participants in radar calibrations.

In the current version of this document, sections or subsections which are directly attributable to one or several sources have been annotated and linked to an extensive list of references found in appendix A. This list is provided primarily as a guide for further reading; a much smaller subset of this list was used in the construction of this document.

TABLE OF CONTENTS

	<u>Page</u>
PREFACE.....	iii
CHAPTER 1	
INTRODUCTION.....	1-1
CHAPTER 2	
RADAR SYSTEMATIC ERROR MODEL DEFINITION.....	2-1
2.1 RANGE COMPONENT.....	2-1
2.2 AZIMUTH COMPONENT.....	2-2
2.3 ELEVATION COMPONENT.....	2-3
2.4 DOPPLER RANGE RATE COMPONENT.....	2-4
CHAPTER 3	
RADAR SYSTEMATIC ERROR MODEL DESCRIPTION.....	3-1
3.1 RANGE COMPONENT.....	3-1
3.1.1 Zeroset and Pulse Width/Bandwidth Mismatch.....	3-1
3.1.1.1 Error Definition and Effects.....	3-1
3.1.1.2 Mathematical Form.....	3-1
3.1.1.3 Measurement.....	3-1
3.1.2 Time Delay and Velocity Servo Lag.....	3-2
3.1.2.1 Error Definition and Effects.....	3-2
3.1.2.2 Mathematical Form.....	3-2
3.1.2.3 Measurement.....	3-2
3.1.3 Acceleration Servo Lag.....	3-2
3.1.3.1 Error Definition and Effects.....	3-2
3.1.3.2 Mathematical Form.....	3-2
3.1.3.3 Measurement.....	3-3
3.1.4 Beacon Delay.....	3-3
3.1.4.1 Error Definition and Effects.....	3-3
3.1.4.2 Mathematical Form.....	3-3
3.1.4.3 Measurement.....	3-3
3.1.5 Transit Time.....	3-3
3.1.5.1 Error Definition and Effects.....	3-3
3.1.5.2 Mathematical Form.....	3-4
3.1.5.3 Measurement.....	3-4
3.1.6 Refraction and Residual Refraction.....	3-4
3.1.6.1 Error Definition and Effects.....	3-4
3.1.6.2 Mathematical Form.....	3-4
3.2 AZIMUTH COMPONENT.....	3-5
3.2.1 Zeroset (or Static Error).....	3-5
3.2.1.1 Error Definition and Effects.....	3-5

TABLE OF CONTENTS (CONT'D)

		<u>Page</u>
3.2.1.2	Mathematical Form.....	3-5
3.2.1.3	Measurement.....	3-5
3.2.2	Time Delay and Velocity Servo Lag.....	3-5
3.2.2.1	Error Definition and Effects.....	3-6
3.2.2.2	Mathematical Form.....	3-6
3.2.2.3	Measurement.....	3-6
3.2.3	Acceleration Servo Lag.....	3-6
3.2.3.1	Error Definition and Effects.....	3-6
3.2.3.2	Mathematical Form.....	3-7
3.2.3.3	Measurement.....	3-7
3.2.4	Pedestal Mislevel and Bearing Wobble (Azimuth Axis Roller Path).....	3-7
3.2.4.1	Error Definition and Effects.....	3-7
3.2.4.2	Mathematical Form.....	3-8
3.2.4.3	Measurement.....	3-8
3.2.5	Transit Time.....	3-8
3.2.5.1	Error Definition and Effects.....	3-8
3.2.5.2	Mathematical Form.....	3-8
3.2.5.3	Measurement.....	3-9
3.2.6	Nonorthogonality (Standards).....	3-9
3.2.6.1	Error Definition and Effects.....	3-9
3.2.6.2	Mathematical Form.....	3-9
3.2.6.3	Measurement.....	3-9
3.2.7	Encoder Nonlinearity.....	3-10
3.2.7.1	Error Definition and Effects.....	3-10
3.2.7.2	Mathematical Form.....	3-11
3.2.7.3	Measurement.....	3-11
3.2.8	Electrical Misalignment (Collimation).....	3-12
3.2.8.1	Error Definition and Effects.....	3-12
3.2.8.2	Mathematical Form.....	3-12
3.2.8.3	Measurement.....	3-12
3.2.9	Vertical Deflection.....	3-13
3.2.9.1	Error Definition and Effects.....	3-13
3.2.9.2	Mathematical Form.....	3-14
3.2.9.3	Measurement.....	3-14
3.3	ELEVATION COMPONENT.....	3-14
3.3.1	Zeroset (or Static Error).....	3-14
3.3.1.1	Error Definition and Effects.....	3-14
3.3.1.2	Mathematical Form.....	3-15
3.3.1.3	Measurement.....	3-15
3.3.2	Time Delay and Velocity Servo Lag.....	3-15
3.3.2.1	Error Definition and Effects.....	3-15
3.3.2.2	Mathematical Form.....	3-15
3.3.2.3	Measurement.....	3-16
3.3.3	Acceleration Servo Lag.....	3-16
3.3.3.1	Error Definition and Effects.....	3-16
3.3.3.2	Mathematical Form.....	3-16

TABLE OF CONTENTS (CONT'D)

		<u>Page</u>
3.3.3.3	Measurement.....	3-16
3.3.4	Pedestal Mismatch and Bearing Wobble (Azimuth Axis Roller Path).....	3-17
3.3.4.1	Error Definition and Effects.....	3-17
3.3.4.2	Mathematical Form.....	3-17
3.3.4.3	Measurement.....	3-17
3.3.5	Transit Time.....	3-17
3.3.5.1	Error Definition and Effects.....	3-18
3.3.5.2	Mathematical Form.....	3-18
3.3.5.3	Measurement.....	3-18
3.3.6	Encoder Nonlinearity.....	3-18
3.3.6.1	Error Definition and Effects.....	3-18
3.3.6.2	Mathematical Form.....	3-19
3.3.6.3	Measurement.....	3-19
3.3.7	Antenna Droop.....	3-20
3.3.7.1	Error Definition and Effects.....	3-20
3.3.7.2	Mathematical Form.....	3-20
3.3.7.3	Measurement.....	3-20
3.3.8	Vertical Deflection.....	3-21
3.3.8.1	Error Definition and Effects.....	3-21
3.3.8.2	Mathematical Form.....	3-22
3.3.8.3	Measurement.....	3-22
3.3.9	Refraction and Residual Refraction.....	3-22
3.3.9.1	Error Definition and Effects.....	3-22
3.3.9.2	Mathematical Form.....	3-22
3.3.9.3	Measurement.....	3-22
3.4	DOPPLER RANGE RATE COMPONENT.....	3-23
3.4.1	Transit Time.....	3-23
3.4.1.1	Error Definition and Effects.....	3-23
3.4.1.2	Mathematical Form.....	3-23
3.4.1.3	Measurement.....	3-23
3.4.2	Time Delay and Acceleration Servo Lag.....	3-23
3.4.2.1	Error Definition and Effects.....	3-24
3.4.2.2	Mathematical Form.....	3-24
3.4.2.3	Measurement.....	3-24
3.4.3	Jerk Servo Lag.....	3-24
3.4.3.1	Error Definition and Effects.....	3-24
3.4.3.2	Mathematical Form.....	3-24
3.4.3.3	Measurement.....	3-25
3.4.4	Refraction and Residual Refraction.....	3-25
3.4.4.1	Error Definition and Effects.....	3-25
3.4.4.2	Mathematical Form.....	3-25
3.4.4.3	Measurement.....	3-25

TABLE OF CONTENTS (CONT'D)

		<u>Page</u>
CHAPTER 4		
	RADAR SYSTEMATIC ERROR MODEL DERIVATION.....	4-1
4.1	RADAR SYSTEM ERRORS.....	4-1
4.1.1	Static Errors.....	4-1
4.1.2	Servo Lag.....	4-2
4.1.3	Pedestal Mismatch.....	4-3
4.1.4	Electrical Misalignment (Collimation).....	4-5
4.1.5	Nonorthogonality (Standards).....	4-6
4.1.6	Encoder Nonlinearity.....	4-8
4.1.7	Antenna Droop.....	4-9
4.1.8	Vertical Deflection.....	4-10
4.2	ATMOSPHERIC ERRORS.....	4-13
4.2.1	Refraction Technical Description.....	4-13
4.2.1.1	REEK Refraction.....	4-14
4.2.1.2	Differential Equation of a Ray (Spherically Stratified Case).....	4-15
4.2.1.3	Range and Elevation Refraction Correction..	4-19
4.2.1.3.1	Range Bending Correction.....	4-19
4.2.1.3.2	Range Retardation Correction.....	4-21
4.2.1.3.3	Total Range Correction.....	4-21
4.2.1.3.4	Elevation Angle Correction.....	4-21
4.2.1.4	Solution to the Differential Equations (Ray Trace).....	4-23
4.2.2	Beacon Delay.....	4-23
CHAPTER 5		
	APPLICATION OF ERROR MODEL.....	5-1
APPENDIX A		
	RELATED DOCUMENTS.....	A-1
ENDNOTES		

TABLE OF CONTENTS (CONT'D)

LIST OF FIGURES

<u>Figure No.</u>		<u>Page</u>
4-1	Mislevel geometry.....	4-3
4-2	Electrical misalignment geometry.....	4-6
4-3	Nonorthogonality geometry.....	4-7
4-4	Encoder nonlinearity geometry.....	4-8
4-5	Droop geometry.....	4-9
4-6	Vertical deflection.....	4-11
4-7	Geometry of observed input.....	4-14
4-8	Geometry of true input.....	4-15
4-9	Definition of terms.....	4-16
4-10	Relationship for bending.....	4-18
4-11	Derivation of bending error.....	4-19
4-12	Geometry for elevation correction.....	4-21

CHAPTER 1

INTRODUCTION

Advancements in missile and space vehicle technology have generated stringent accuracy requirements for instrumentation tracking radars. Because these radars make precise measurements of the location of a test object in space, such measurements must be calibrated to a common or accepted reference to establish the accuracy of the measurements obtained.² The Joint Range Instrumentation Accuracy Improvement Group (JRIAIG) of the Range Commanders Council (RCC) surveyed the range community to determine whether or not radar calibrations were being done, and if so, what procedures were being followed and what error models were being used. The response to this survey showed that excellent radar calibration procedures have been developed by several ranges and that the error models now in use are nearly identical. Each participating range submitted copies of the radar calibration procedures in use at its ranges as contributions to the construction of this document. Although the specifics of the procedures may deviate from one range to another, the theory and general techniques are the same.

The effort from this point has focused mainly upon identifying the error terms in common use at all ranges and restructuring the standard error model to reflect these similarities. In section 2, the radar error model is defined in terms of range, azimuth, elevation, and doppler range-rate errors. In section 3, these terms are further explained with some high-level descriptions of the common methods of measurement. Section 4 provides derivations for the individual error model elements, while section 5 covers error coefficient collection methodology. In this version of the catalog, no attempt has been made to specifically address individual types of radar systems. Instead, measurement procedures are described in general terms, focusing on the nature of the measurement rather than the details.

This document does not provide discussion of all radar error sources identified by other IRIG documents but rather addresses those major error sources for which mathematical models exist and calibration procedures have been developed. Earlier documents (IRIG Document 117-69, February 1969; PMR-JRIAIG Documents 1-73, May 1976 and 20-73, April 1976) discuss a very large number of terms applied in known radar error models; however, the abbreviated list of terms addressed in this document account for better than 90 percent of the systematic errors contained in most radar data. The remaining 10 percent of the terms, either cannot be estimated and removed or result from random and undetermined

error sources. The goal of the error model is to maintain the total contribution of uncorrected systematic errors to less than one least significant bit (LSB) for the instrument in question.

This document summarizes information about existing calibration procedures, so any range can use this document to tailor its procedures. The individual error model terms themselves are presented as errors which are subtracted from the measured data to yield corrected data and to represent the relationship between the true and measured data as in

$$\text{Error} = \text{Measured} - \text{True}$$

While using the error model, particular attention should be given to the relationship between the physical meaning of the error source and the sign convention of its correction. Moreover, the term normal refer to azimuth and elevation values recorded when the measured elevation is less than 90° (0 to 90°). The term plunge refers to those values recorded when elevation is greater than 90° (90 to 180°). The azimuth value is undetermined at 90° elevation and will cause difficulty in the error model application.

CHAPTER 2

RADAR SYSTEMATIC ERROR MODEL DEFINITION

The term "error model" can be misleading. The implication can be that the true position or state of a target is known and that, when the measured values are compared to the truth, errors are found which can be modeled. In reality, the exact location of the target is unknowable; however, for practical applications, truth standards can be any source of information that is sufficiently more accurate than the system being calibrated. Often, an order of magnitude is used as the criterion for a data source to function as the truth standard; that is, the true-to-measured accuracy ratio is greater than ten. Under these conditions, comparison of the measured data with the truth standard yields error residuals that reflect the combined effect of both systematic and random errors in the measurement. The error model describes known systematic errors which can be mathematically subtracted from the data. The total correctable error is the resultant superposition of all the systematic error terms, and these are divided among the four separate components of range, azimuth, elevation, and Doppler range rate. A fifth component, phase derived range (range vernier), will not be discussed. Each term will be addressed in section 3 with derivations to follow in section 4.

2.1 RANGE COMPONENT

$$R_c = R_o$$

- a_0 Zeroset
- a'_0 Pulse Width/Bandwidth Mismatch
- $a_1 \dot{R}_e$ Time Delay
- $a'_1 \dot{R}_e$ Velocity Servo Lag ($a'_1 = 1/K_v^R$)
- $a_2 \ddot{R}_e$ Acceleration Servo Lag ($a_2 = 1/K_a^R$)
- $a_3 \cdot f(S/N)$ Beacon Delay

- + $a_4 R_1 \dot{R}_e$ Transit Time ($a_4 = 1 / \text{speed of light}$)
- $a_5 X / R_1$ X Survey
- $a_6 Y / R_1$ Y Survey
- $a_7 Z / R_1$ Z Survey
- ρ_R Refraction
- ρ'_R Residual Refraction

2.2 AZIMUTH COMPONENT

$$A_c = A_o$$

- b_o Zeroseat
- $b_1 \dot{A}_e$ Time Delay
- $b'_1 \ddot{A}_e$ Velocity Servo Lag ($b'_1 = 1/K_v$)
- $b_2 \ddot{A}_e$ Acceleration Servo Lag ($b_2 = 1/K_a$)
- $b_3 \sin (A_1 + \alpha_1) \tan E_2$ Misllevel
- $b_4 \sin (2A_1 + \alpha_2) \tan E_2$ Misllevel Wobble
- $b_5 R_1 \dot{A}_e$ Transit Time ($b_5 = 1 / \text{speed of light}$)
- $b_6 \tan E_2$ Nonorthogonality (Standards)
- $b_7 \cos (m_1 A_o + \phi_1)$ m_1 Harmonic Encoder Nonlinearity
- $b_8 \cos (m_2 A_o + \phi_2)$ m_2 Harmonic Encoder Nonlinearity
- $b_9 \cos (m_3 A_o + \phi_3)$ m_3 Harmonic Encoder Nonlinearity

- $b_{10} \sec E_2$ Electrical Misalignment (Collimation)
- $\eta \tan \phi - \eta \tan E_2 \cos A_2 + \xi \tan E_2 \sin A_2$.. Vertical Deflection
- $a_5 \frac{\cos A_2 \sec E_2}{R_1}$ X Survey
- $a_6 \frac{\sin A_2 \sec E_2}{R_1}$ Y Survey

2.3 ELEVATION COMPONENT

$$E_c = E_o$$

- c_o Zeroset
- $c_1 \dot{E}_o$ Time Delay
- $c_1' \dot{E}_o$ Velocity Servo Lag ($c_1' = 1/K_v^E$)
- $c_2 \ddot{E}_o$ Acceleration Servo Lag ($c_2 = 1/K_a^E$)
- $c_3 \cos (A_1 + \beta_1)$ Mislevel
- $c_4 \cos (2A_1 + \beta_2)$ Mislevel Wobble
- $c_5 R_1 \dot{E}_o$ Transit Time ($c_5 = 1/\text{speed of light}$)
- $c_6 \cos (n_1 E_o + \theta_1)$ n_1 Harmonic Encoder Nonlinearity
- $c_7 \cos (n_2 E_o + \theta_2)$ n_2 Harmonic Encoder Nonlinearity
- $c_8 \cos (n_3 E_o + \theta_3)$ n_3 Harmonic Encoder Nonlinearity
- $c_9 \cos E_1$ Antenna Droop

- $\eta \sin A_2 + \zeta \cos A_2$ Vertical Deflection
- $a_6 \frac{\sin A_2 \sin E_2}{R_1}$ X Survey
- $a_6 \frac{\cos A_2 \sin E_2}{R_1}$ Y Survey
- $a_7 \frac{\cos E_2}{R_1}$ Z Survey
- ρ_E Refraction
- ρ'_E Residual Refraction

2.4 DOPPLER RANGE RATE COMPONENT

$$\dot{R}_c = \dot{R}_D$$

- $d_1 R_1 \dot{R}_c$ Transit Time ($d_1 = 1 / \text{speed of light}$)
- $d_2 \ddot{R}_c$ Time Delay ($d_2 = 1/K_1^D$)
- $d_2' \ddot{R}_c$ Acceleration Servo Lag ($d_2' = 1/K_1^D$)
- $d_3 \ddot{R}_c$ Jerk Servo Lag
- ρ_{RR} Refraction
- ρ'_{RR} Residual Refraction

where

$$R_1 = R_0 - a_0$$

$$A_1 = A_0 - b_0 - b_7 \cos (m_1 A_0 + \phi_1) - b_8 \cos (m_2 A_0 + \phi_2) - b_9 \cos (m_3 A_0 + \phi_3)$$

$$A_2 = A_1 - b_{10} \sec E_2 - b_6 \tan E_2 - \{b_3 \sin (A_1 + \alpha_1) - b_4 \sin (2A_1 + \alpha_2)\} \tan E_2$$

$$E_1 = E_0 - c_0 - c_6 \cos (n_1 E_0 + \theta_1) - c_7 \cos (n_2 E_0 + \theta_2) - c_8 \cos (n_3 E_0 + \theta_3)$$

$$E_2 = E_1 - c_9 \cos E_1 - c_3 \cos (A_1 + \beta_1) - c_4 \cos (2A_1 + \beta_2)$$

and

R_c = Corrected Range

A_c = Corrected Azimuth

E_c = Corrected Elevation

\dot{R}_c = Corrected Doppler Range Rate

R_0 = Measured Range

\dot{R}_0 = Estimated Range Velocity

\ddot{R}_0 = Estimated Range Acceleration

R_j = Estimated Range Jerk

A_0 = Measured Azimuth

\dot{A}_0 = Estimated Azimuth Velocity

\ddot{A}_0 = Estimated Azimuth Acceleration

E_0 = Measured Elevation

\dot{E}_e = Estimated Elevation Velocity

\ddot{E}_e = Estimated Elevation Acceleration

\dot{R}_0 = Measured Doppler Range Rate

α_1, β_1 = Mislevel Phase Angle

α_2, β_2 = Mislevel Wobble Phase Angle

ξ, η = Vertical Deflection Components

ϕ_A = Astronomic Latitude of Radar System

ρ_R = Range Refraction Correction

ρ'_R = Range Residual Refraction Correction

ρ_E = Elevation Refraction Correction

ρ'_E = Elevation Residual Refraction Correction

ρ_{RR} = Doppler Range Rate Refraction Correction

ρ'_{RR} = Doppler Range Rate Residual Refraction Correction

m_1, m_2, m_3 = Harmonics for Azimuth Nonlinearity

n_1, n_2, n_3 = Harmonics for Elevation Nonlinearity

ϕ_1, ϕ_2, ϕ_3 = Azimuth Nonlinearity Phase Angles

$\theta_1, \theta_2, \theta_3$ = Elevation Nonlinearity Phase Angles

a_i, b_i, c_i, d_i = Coefficients of Systematic Error Corrections

CHAPTER 3

RADAR SYSTEMATIC ERROR MODEL DESCRIPTION

In this section, the foregoing error model equations are discussed in further detail. Where practical, a one-to-one correspondence has been maintained between the error terms presented in section 2 and those described in section 3. Derivations are presented in section 4. This section is subdivided into the four error components of range, azimuth, elevation, and doppler range rate.

3.1 RANGE COMPONENT

3.1.1 Zeroset and Pulse Width/Bandwidth Mismatch. This term accounts for the constant range error induced by various effects specific to the particular ranging system in use.

3.1.1.1 Error Definition and Effects. Range zeroset generally refers to constant errors in the range measurement because of such variable factors as tuning and calibration. In the broader definition, range zeroset may also incorporate errors caused by transponder delay setting errors, pulse width or bandwidth mismatch. The effect on the output range data is a constant bias which may vary noticeably from mission to mission.

3.1.1.2 Mathematical Form. The various error elements of range zeroset are folded into a single variable, a_0 , representing the total combined constant bias. In some applications, the error contribution from pulse width/bandwidth mismatch is separated from other zeroset terms, which is designated by the coefficient, a'_0 .

$$\left| \begin{array}{l} \Delta R = a_0 \quad \text{Zeroset} \\ \Delta R = a'_0 \quad \text{Pulse Width/Bandwidth Mismatch} \end{array} \right.$$

3.1.1.3 Measurement. Range zeroset is generally determined by locking onto a passive reflector located at a known distance or by range calibrators designed to zeroset range systems. In this procedure, the surveyed distance (refraction corrected) minus the radar-measured distance will yield the range zeroset. It is important to note the use of a passive reflector can result in errors from various sources such as low-elevation signal multi-path, inaccurate refraction correction, or pulse width/bandwidth mismatch. Zeroset may also be determined by tracking a target

with known trajectory but may be complicated because of scintillation or beacon delay. Range calibrations can reduce errors from many of the above sources.

3.1.2 Time Delay and Velocity Servo Lag. Velocity servo lag describes an error condition resulting from a target's motion which is not applicable to most modern radar systems. Time delay reflects an actual bias in the radar's timing which is identical to velocity servo lag in its effect on the range measurement.

3.1.2.1 Error Definition and Effects. Velocity servo lag in the range component refers to an older type of radar-ranging system in which type 1 servos were used to determine range. An error results from the range system's inability to respond to the motion of a target along the line between the radar and the target. Time delay is unrelated to the range servos but shares the same functional form.

3.1.2.2 Mathematical Form. If applicable, the next equation will account for velocity servo lag and time delay effects. If not applicable, a_1 and a'_1 may be set to zero in the radar error model equation.

$$\begin{array}{l} \Delta R = a_1 \dot{R}_e \quad \text{Time Delay} \\ \Delta R = a'_1 \dot{R}_e \quad \text{Velocity Servo Lag} \end{array}$$

3.1.2.3 Measurement. Measurement of the velocity servo lag is radar specific and will not be addressed. Time delay is also a radar (or range) specific error condition and should be determined according to applicable procedures. If a truth standard (satellite of known trajectory) is available, then the time delay (if any) may be obtained from the slope of a plot of the range residuals versus range rate.

3.1.3 Acceleration Servo Lag. Acceleration servo lag describes an error condition caused by the motion of a target accelerating with respect to the radar.

3.1.3.1 Error Definition and Effects. Acceleration servo lag in the range component results from the range system's inability to respond to the motion of a target which is accelerating along the line between the target and the radar. The effects are reduced by operator bandwidth switching.

3.1.3.2 Mathematical Form. If applicable, the next equation will account for acceleration servo lag. If not applicable, a_2 may be set to zero in the radar error model equation.

$$\Delta R = a_2 \ddot{R}_e$$

3.1.3.3 Measurement. Measurement of the acceleration servo lag is radar specific and will not be addressed.

3.1.4 Beacon Delay. This term accounts for the difference between the actual range of a target and the radar's measured beacon-mode range to the target. This difference is caused by the target's transponder.

3.1.4.1 Error Definition and Effects³. A beacon is a transponder mounted on the target which receives the radar pulse, interprets the signal for proper interrogation identity, and transmits a return pulse after a preset amount of time known as the delay. For calibration purposes, beacon delay is commonly divided into two contributing factors: fixed delay and delay variation. Fixed delay is generally known prior to a mission and can be incorporated into the range system of the radar. Delay variation changes as a function of the signal strength detected by the beacon receiver. The combined effect of both factors will yield a range value which is long or short depending on the nature of the error.

3.1.4.2 Mathematical Form. In the beacon-delay equation, α represents the fixed delay. The variable, a_3 , is the desired coefficient of beacon delay.

$$|\Delta R = \alpha + a_3 \cdot f(S/N)$$

3.1.4.3 Measurement. The fixed-beacon delay can sometimes be measured by the radar system when the beacon is located at a known range (surveyed position). In this approach, the known range is subtracted from the measured range, and the difference (beacon delay) is set in the system prior to an operation or incorporated during post-flight analysis. If the beacon is mounted on an aircraft in the configuration used for flight operations, then delays associated with cabling between the beacon antenna and beacon receiver can be removed as well. The fixed-beacon delay can also be measured in a laboratory and provided to the radar site prior to tracking. Determination of the delay variation is more difficult, because the received signal strength at the beacon is not always known. Estimates of the signal-level curve may be appropriate, however.

3.1.5 Transit Time. This term accounts for the range error induced by the motion of the target as the reflected (or transmitted) radar pulse travels from the target at the finite speed of light. This error is typically only significant for great distances and velocities.

3.1.5.1 Error Definition and Effects. Transit time errors arise because radar electromagnetic energy travels at a finite speed and cannot report the instantaneous position of the target.

During a mission, the radar transmits a pulse which is then returned from the target either by beacon transmission or reflection. In the time that it takes for that return signal to travel back to the radar, the target will have moved a distance equal to the velocity of the target times the transit time of the signal. Consequently, at the time a radar measurement is completed, the target has moved to a new position, and a measurement error is present.

3.1.5.2 Mathematical Form. The transit-time equation assumes that range deltas and time intervals are sufficiently small to accurately approximate range rate. The estimated range velocity is derived from the measured range value, and a_r represents the reciprocal of the speed of light.

$$|\Delta R = a_r R \dot{R}_e$$

The use of the vacuum speed of light for trans-atmospheric purposes is a valid assumption, because the atmospheric effects are considered in the refraction-error term. Correction of transit-time error can be achieved in one of two ways: by applying the foregoing equation to the measured data or by changing the time tag of the data.

3.1.5.3 Measurement. Since transit time is functionally related to the range and range rate values, the amount of error will vary throughout a mission. There is no fixed transit-time error which can be measured and applied for a radar system. Accuracy is only affected by the selection of a speed of light standard which is accepted by the calibration community and the method by which \dot{R}_e is determined.

3.1.6 Refraction and Residual Refraction. This term accounts for errors induced into range measurement by an inappropriate or inaccurate refraction model correction.

3.1.6.1 Error Definition and Effects. Refraction errors are caused by variations in the propagation velocity of the radar's electromagnetic energy which yield an incorrect range measurement. Residual-refraction errors result from an incorrect assessment or estimate of the refractive index of the atmosphere along the signal path. The ability to properly assess the conditions is limited by the discrete number of observations made, the timeliness of the data, and the refractive anomalies along the propagation path.

3.1.6.2 Mathematical Form. Although presented as a constant, this variable could actually represent any number of functions designed to specifically address shortcomings in the refraction model applied to the data. The danger of such an open-ended approach is that it may actually absorb errors attributable to other systematic error sources during a regression analysis routine.

$$\begin{array}{|l} \Delta R = \rho_R \text{ Refraction} \\ \Delta R = \rho'_R \text{ Residual Refraction} \end{array}$$

3.1.6.3 Measurement. Refraction errors are determined through the use of sophisticated mathematical models based on inputs from the local environment. Residual refraction is intended to address errors associated with inaccurate weather condition inputs to the refraction model.

3.2 AZIMUTH COMPONENT

3.2.1 Zeroset (or Static Error). This term accounts for the constant offset of the measured value from the true value caused primarily by misalignment of the zero point of the azimuth encoder axis.

3.2.1.1 Error Definition and Effects. Azimuth zeroset is the difference between true north and the mechanical azimuth encoder zero position caused by the misalignment of the azimuth encoder axis. Static error is a broader-scoped term which attempts to encompass all constant offset errors in the azimuth data caused by such factors as operator alignment error, misorientation, and alignment flaws. This bias value alters all of the azimuth output data by a fixed amount.

3.2.1.2 Mathematical Form. All offset error sources are combined under the following equation. For purposes of systems analysis, some ranges may elect to subdivide this error term into its individual error elements.

$$|\Delta A = b_0$$

3.2.1.3 Measurement. Using the boresight telescope to track the star, Polaris, the azimuth position is recorded at known times. This value is then compared to a computed value for the position of Polaris, and the misalignment is deduced. By recording these measurements in the normal and plunge position, the need for precise boresight telescope alignment with the radio frequency (RF) axis is eliminated.

3.2.2 Time Delay and Velocity Servo Lag. Velocity servo lag describes the situation in which the radar system is not pointing directly at a dynamically moving target being tracked because of the radar's inability to sufficiently adjust for a tracking error before the angular velocity of the target creates a new tracking error. Time delay indicates an actual bias in the radar's timing, but the effect is identical to that of velocity servo lag.

3.2.2.1 Error Definition and Effects. As the radar system tracks a constant angular velocity target, the servo system responds to the displacement error and continually repositions the antenna to reduce the position error. A target moving with constant azimuth velocity will require the antenna to rotate at a constant azimuth velocity to overcome the position error. The constant error remaining between the actual target position and the antenna position is called a velocity servo lag. Velocity servo lag is only significant for type 1 servo systems; this error is zero for type 2 systems.

3.2.2.2 Mathematical Form. The error constants, b_1 and b'_2 , have the units of time. Multiplied by the azimuth angular velocity, this error coefficient will yield the appropriate angular correction of

$$\begin{array}{l} \Delta A = b_1 \dot{A}, \quad \text{Time Delay} \\ \Delta A = b'_1 \dot{A}, \quad \text{Velocity Servo Lag} \end{array}$$

In field procedures, the velocity servo lag measurement is commonly referred to as K_v . The relationship between b'_1 and K_v is $b'_1 = 1/K_v$.

3.2.2.3 Measurement. Measurement of the velocity servo lag value is radar specific and will not be addressed. Although the procedure performed in its entirety is lengthy and time consuming, many steps need not be repeated each time the velocity servo lag constant is determined. The system's K_v should be checked daily; this check takes approximately 15 minutes. If a truth standard (satellite of known trajectory) is available, the time delay (if any) may be estimated from the plot slope of the azimuth residuals versus azimuth rate.

3.2.3 Acceleration Servo Lag. Acceleration servo lag describes the situation in which the radar system is not pointing directly at a dynamically moving target being tracked because of the radar's inability to sufficiently adjust for a tracking error before the angular acceleration of the target creates a new tracking error.

3.2.3.1 Error Definition and Effects. As the radar system tracks a constantly accelerating target, the servo system must remain on track by continually overcoming the constantly changing velocity of the target. The acceleration constant is a measure of the radar system's ability to maintain track on the accelerating target and is related to the velocity constant. This value will change with each bandwidth setting.

3.2.3.2 Mathematical Form. The acceleration servo lag error constant, b_2 , has the units of time squared. Multiplied by the azimuth angular acceleration, this error coefficient will yield the appropriate angular correction.

$$|\Delta A = b_2 \ddot{A}_e$$

In field procedures, the acceleration servo lag measurement is commonly referred to as K_a . The relationship between b_2 and K_a is $b_2 = 1/K_a$.

3.2.3.3 Measurement. Measurement of the acceleration servo lag value is radar specific and will not be addressed. Although the procedure performed in its entirety is lengthy and time consuming, many steps need not be repeated each time the acceleration servo lag constant is determined. The system's K_a can be determined and recorded on an operational basis for only the bandwidths used during the operation. The K_a recordings can be made within a 20-30 minute period.

3.2.4 Pedestal Mislevel and Bearing Wobble (Azimuth Axis Roller Path). These terms account for the total amount of tilt of the azimuth axis in reference to that of the local vertical. This error is primarily caused by mounting irregularities and thermal gradients within the pedestal. In most cases, bearing wobble does not exist but rather is due to improper location of the levels.

3.2.4.1 Error Definition and Effects⁴. Pedestal mislevel refers to the tilt of the azimuth axis from the local vertical. Azimuth axis roller-path error (bearing wobble) is the result of imperfect azimuth axis bearings. Pedestal mislevel and azimuth axis roller-path errors are discussed here, because they have a similar effect on radar azimuth and elevation-angle error and both are measured in the same procedure. These errors are characterized by the first three harmonics of the cosine function. The first harmonic represents mislevel; the remaining harmonic terms describe the azimuth axis roller-path error. Of these, only the second harmonic is described in the error model. The effect on azimuth is a function of the tangent of the elevation angle and the sine of the azimuth angle plus a phase bias. The azimuth mislevel error becomes pronounced at the higher elevation angles because of the convergence of the azimuth lines at the zenith, but erroneous mislevel values will result from improperly installed equipment or faulty measurements.

3.2.4.2 Mathematical Form. In the mislevel and wobble equations, b_3 and b_4 represent the desired coefficients of amplitude; α_1 and α_2 represent phase angle. A_1 is the measured azimuth corrected for zeroset and encoder nonlinearity. E_2 is the measured elevation corrected for zeroset, encoder nonlinearity, droop, and elevation mislevel component.

$$\begin{cases} \Delta A = b_3 \sin(A_1 + \alpha_1) \tan E_2 & \text{Mislevel} \\ \Delta A = b_4 \sin(2A_1 + \alpha_1) \tan E_2 & \text{Wobble} \end{cases}$$

3.2.4.3 Measurement. Mislevel is generally measured by mounting a level-reading device such as a Talyvel or inclinometer on the radar pedestal and recording readings at uniform intervals throughout a 360° turn of the pedestal. These readings are then fit to a sinusoidal curve to determine amplitude and phase. Depending on resources, the interval may range from a maximum of 90° to a minimum of 0° (continuous). Generally speaking, the gross motion of the pedestal precludes continuous measurements because of vibration. Mislevel may also be determined by fitting a curve to the boresite measurements of several stars throughout a 360° turn.

3.2.5 Transit Time. This term accounts for the azimuth error induced by the motion of the target as the reflected (or transmitted) radar pulse travels from the target at the finite speed of light. This error is typically only significant for great distances and velocities.

3.2.5.1 Error Definition and Effects. Transit time errors arise because radar electromagnetic energy travels at a finite speed and cannot report the instantaneous position of the target. During a mission, the radar transmits a pulse which is then returned from the target either by beacon transmission or reflection. In the time that it takes for that return signal to travel back to the radar, the target will have moved a distance equal to the velocity of the target times the transit time of the signal. At the time of a radar measurement completion, the target has moved to a new position, and a measurement error is present.

3.2.5.2 Mathematical Form. The transit-time equation derives from the assumption that azimuth deltas and time intervals are sufficiently small to accurately approximate azimuth rate. The estimated azimuth velocity derives from the measured azimuth value, and b_5 represents the reciprocal of the speed of light.

$$\Delta A = b_5 R_1 \dot{A}_e$$

The use of the vacuum speed of light for trans-atmospheric purposes is a valid assumption, since the atmospheric effects are considered in the refraction error term. Correction of transit time error can be achieved in one of two ways: by applying the foregoing equation to the measured data or by changing the time tag of the data.

3.2.5.3 Measurement. Since transit time is functionally related to the range and azimuth rate values, the amount of error will vary throughout a mission. There is no fixed transit-time error which can be measured and applied for a radar system. Accuracy is only affected by the selection of a speed of light standard which is accepted by the calibration community and the method by which Δ is determined.

3.2.6 Nonorthogonality (Standards). This term accounts for the measured azimuth error induced by the tilt of the elevation rotation axis from orthogonality with the azimuth rotation axis.

3.2.6.1 Error Definition and Effects⁴. The elevation axis is supported by the standards. In an ideal 2-axis gimbal azimuth/elevation tracking mount, the elevation axis of rotation is orthogonal (perpendicular in 3-space) to the azimuth axis of rotation. Because of pedestal fabrication, assembly, and tooling jig misalignments inherent in the manufacturing process, the standards will not support each end of the elevation axis at the same height above the azimuth plane. As a result, an azimuth-measurement error will be present and increase as a function of elevation angle. In a dynamic situation, the RF axis will require a rotation of the azimuth platform to maintain target track which increases in elevation but maintains constant azimuth.

3.2.6.2 Mathematical Form. Through the principles of spherical trigonometry, the nonorthogonality error equation is derived to show that the effect on azimuth is proportional to the tangent of the elevation angle. An upward tilt of the right side of the elevation axis, as viewed by an observer behind the radar, causes a positive error in the azimuth data output. The coefficient, b_6 , represents the angle of nonorthogonality; E_2 assumes no zero set, droop, or mislevel errors in the measured elevation angle.

$$|\Delta A = b_6 \tan E_2$$

This error can significantly affect the azimuth data, but it has negligible effect on elevation angle data.

3.2.6.3 Measurement⁴. No provision exists for the physical correction of this error after initial assembly of the pedestal; consequently, it is necessary to periodically measure this error

in the field. The nonorthogonality coefficient is generally a fixed value which, once established, only requires further measurement to determine seasonal fluctuations (thermal expansion) and long-term bearing wear.

Nonorthogonality can also be stated as the amount of non-parallelism between the elevation axis and the azimuth plane of rotation; it is with respect to this equivalent definition that the following test actually measures nonorthogonality. A Talyvel electronic level, capable of measuring level indications to one arc-second or better, is used to establish the azimuth plane of rotation. A second Talyvel unit is mounted on an AA Gage ULTRADEX connected to the RF head between the elevation axis bearings. A level curve is taken at 400 mil increments of azimuth, reading both units. One data pass is taken with the elevation of the antenna at zero, and the other data pass is taken with the antenna in the plunge position. In going from the normal to plunge position, the axis mounted level unit becomes inverted by 180° plus twice the magnitude of the nonorthogonality error. A change to the upright position is accomplished by an exact 180° rotation of the ULTRADEX, leaving the two data passes biased by twice the magnitude of the nonorthogonality. Several data passes are taken to determine precision of the measurement.

3.2.7 Encoder Nonlinearity. A precision-shaft angle encoder is a device which translates the mechanical rotation of a shaft into an incremental electrical digital representation. This term accounts for inaccuracies in the azimuth data output resulting from deviations in the straight line correlation of the input shaft rotation and the incremental output electrical digital representation because of various factors such as environmental conditions, inherent system errors, loading, and misalignment effects.

3.2.7.1 Error Definition and Effects⁴. The error produced is the difference between the encoder output and the actual azimuth axis angular position resulting from misalignment in the mechanical linkage or manufacturing defects. The error is systematic and represents a nonlinear functional change which can be represented by an n-order harmonic series. Experience has indicated that, for a direct drive encoder coupling, measured nonlinearities for the first harmonic are very small and can usually be ignored. In most cases, the second harmonic is not related to the encoder but rather is induced by the operator during the test setup. The nonlinearity of the azimuth encoder causes a variable bias to be introduced into the azimuth output data. Although the effect would be relatively small at close range, the magnitude of the error could become quite significant at long range.

The encoder coupling misalignment error has a complex relationship to the input angle. The three components considered are

- axial translation,
- radial translation from concentricity, and
- angle between rotational axes.

Each of these contributions to the coupling error is a function of the shaft angle position. These functions usually possess a periodicity equal to some submultiple of 360° but may have different average values and arbitrary phase relationships with respect to the input angles. Other error sources such as velocity, acceleration, and temperature exist but are not specifically addressed. Some radars (FPS-16) may employ older systems where a coarse and fine encoder are used. Large errors in the 16th and 32d harmonics are commonly found in these systems.

3.2.7.2 Mathematical Form. The nonlinearity error effect causes a varying azimuth angle output bias which follows the cosine of the azimuth shaft angle change. The azimuth zeroset and collimation-error measurements must be considered when encoder data is used for nonlinearity error determination purposes.

$$\begin{array}{l} \Delta A = b_7 \cos (m_1 A_o + \phi_1) \quad m_1 \text{ Harmonic} \\ \Delta A = b_8 \cos (m_2 A_o + \phi_2) \quad m_2 \text{ Harmonic} \\ \Delta A = b_9 \cos (m_3 A_o + \phi_3) \quad m_3 \text{ Harmonic} \end{array}$$

In the foregoing equation, b_7 , b_8 , and b_9 are the coefficients representing the amplitudes of the harmonic error, while ϕ_1 , ϕ_2 , and ϕ_3 represent the phase angles. The variables m_1 , m_2 , and m_3 indicate the harmonic number; while they are indicated here as representing the first three harmonics, they may in practice represent any combination of harmonics.

3.2.7.3 Measurement⁴. The testing of a precision-angle encoder of any type should take into account all aspects of system performance as well as the interface between the encoder and the system with which it will be used. Measurement of the encoder nonlinearity is dependent upon the particular type and brand of encoding system. In general, the encoder output angle increment is compared against a precisely measured (via ULTRADEX, auto-collimator, or similar) shaft angle increment through a turn of 360° in azimuth. The recorded deviations of the encoder output from the true rotation are then modeled with the cosine series as discussed. The deviations will represent the summation of all contributing harmonics; therefore, caution must be exercised when attempting to model the function.

Static accuracy or resolution is a measure of the encoder's ability to correlate an infinitesimal rotation of the shaft with the transition from one encoder quantum state to another. Encoder resolution is equal to the number of quantized positions per turn of the input shaft. It contributes an uncertainty to the system output which is a fraction of the smallest quantum, known as the least significant bit (LSB) and is equal to one-half a quantum in the worst case. The quantum transition state is evidenced by the 'togglng' of the LSB from one number to the next and back again in a continuing rapid fluctuation.

3.2.8 Electrical Misalignment (Collimation). This term accounts for the measured azimuth error induced by the misalignment of the mechanical and RF axes.

3.2.8.1 Error Definition and Effects. The RF axis of the radar is intended to be coincident with the mechanical axis of the radar as defined by the azimuth and elevation encoders (assuming all necessary corrections). In practice, however, there is some misalignment error caused by mechanical, optical, or electrical effects. Mechanical misalignment results from an imperfect parabolic reflecting plane or improper orientation of the feed horn assembly causing noncolinearity of the RF and mechanical axes.⁵ Optical misalignment results from a nonparallel alignment of the optical and mechanical axes causing a constant bias if the optical axis is used to calibrate the electrical axis. Electrical misalignment results from an improper phase adjustment in the receiving system which causes an apparent shift of the RF axis from the mechanical axis. The misalignment can be decomposed into two perpendicular components: one along the elevation circle and the other perpendicular to the plane of the elevation circle.

3.2.8.2 Mathematical Form. Through the use of spherical trigonometry, the effect of electrical misalignment on the azimuth measurement is shown to be functionally related to the secant of the elevation. The coefficient, b_{10} , represents the actual angular separation (azimuth component) of the electrical and mechanical axes.

$$|\Delta A = b_{10} \sec E_2$$

The elevation component of electrical misalignment is constant and, therefore, absorbed into the elevation zero set coefficient.

3.2.8.3 Measurement. Azimuth error caused by electrical misalignment should be determined on a pre-operational test-by-test basis. This error term is sensitive to mission polarization mode and received mission frequency. Satellite tracks are generally more desirable in determining this error, but the following example of collimation measurement will provide quick results using only a few data points.

Most static RF axis misalignment measurement procedures consist of pointing the radar electrically toward a fixed point in the normal position. Normal radar orientation is when the radar is directed toward a target with the elevation angle reading less than 90° . After recording the normal azimuth angle, the radar is plunged (elevation angle greater than 90°) and rotated in azimuth until it again electrically locks onto the same point in space. Because of the geometry of the rotations, the amount of necessary deviation from a 180° rotation is double the amount by which the RF axis is not perpendicular to the elevation axis (azimuth component). If the RF axis is perpendicular to the elevation axis, the azimuth rotation required to rotate the radar to lock on in the plunge position will be exactly 180° .

3.2.9 Vertical Deflection. This term accounts for the azimuth difference induced by the misalignment of the local gravity vector from the normal vector of the ellipsoid reference model.

3.2.9.1 Error Definition and Effects. Strictly speaking, the deflection of the vertical is not an error in the radar measurement. Radar measurements must be made with respect to a coordinate system, and many radars use the astronomic vertical as an axis in their system. Radars that have their vertical axis aligned with the astronomic vertical make their measurements in an apparent or astronomic topocentric system referenced to the earth's geoid. While trajectory computations are most often performed on a mathematical ellipsoid such as DOD World Geodetic System 1984 (WGS-84), which closely approximates the size and shape of the geoid. The ellipsoid is a mathematically defined regular surface with specific dimensions. The geoid coincides with the surface to which the oceans would conform over the entire earth if free to adjust to the combined effect of the earth's mass attraction and the centrifugal force of the earth's rotation. As a result of the uneven distribution of the earth's mass, the geoidal surface is irregular. Since the ellipsoid is a regular surface, the two will not coincide. The areas of separation between the geoid and ellipsoid are referred to as geoid undulations, geoid heights, or geoid separations.

The geoid is a surface where the gravity potential is equal everywhere and where the gravity vector is always perpendicular. The angle between the perpendicular to the geoid (plumb line) and the perpendicular to the ellipsoid is defined as the deflection of the vertical. The vertical deflection angle is usually resolved into a north-south component which is coincident with the local meridian and equal to the difference between astronomic and geodetic latitude and an east-west component which is coincident with the prime vertical and proportional to the difference between astronomical and geodetic longitude. The north-south and east-west components of vertical deflection are referenced by the U.S. Geological Survey as ξ and η , with a north, south, east, or

west identifier to indicate the direction in which the astronomic zenith is deflected relative to the geodetic zenith as viewed from a point in space. Thus, the correction for vertical deflection is really a coordinate system transformation from the astronomic topocentric to the geodetic topocentric coordinate system.

This transformation is determined by processing requirements and, in some cases, will lead to data degradation as a result of computer round off. Typically, this transformation is made because users of the radar data want it referenced to specific earth models such as WGS-84, or it will be combined with other instrumentation and the final trajectory estimate referenced to a specific earth model.

3.2.9.2 Mathematical Form. The equation describing vertical deflection uses the north-south and east-west components provided by the U.S. Geological Survey. The following equation provides the azimuth error as a function of azimuth and elevation. There are no coefficients to be determined. A_2 and E_2 are the adjusted azimuth and elevation angles of measurement, and ϕ_A is the astronomic latitude of the radar station.

$$|\Delta A = \eta \tan \phi_A - \eta \tan E_2 \cos A_2 + \xi \tan E_2 \sin A_2$$

Confusion with the polarity of the variables of vertical deflection generally arises from the local sign convention. A review of local procedures is warranted to ensure proper use of this error term, particularly in regions of the world where vertical deflection is significantly large.

3.2.9.3 Measurement. Although measurement by each range is possible, it is generally better to use the values provided by the Defense Mapping Agency (DMA).

3.3 ELEVATION COMPONENT

3.3.1 Zeroset (or Static Error). This term accounts for the constant offset of the measured elevation angle from true caused by misalignment of the elevation encoder axis, RF collimation shift in the elevation plane, or both.

3.3.1.1 Error Definition and Effects. Elevation zeroset can represent two different types of constant offset. In the first representation, zeroset defines the mechanical offset of the encoder zero point from the true zero point. In the second representation, zeroset (or static error) defines the total offset error as a combination of the mechanical offset and the RF collimation offset. The first definition is useful for encoder alignment, while the second definition is useful (and necessary)

for correction of measured data. The effect on the measured data of both definitions is a constant bias from the true position.

3.3.1.2 Mathematical Form. All offset error sources are combined under the following equation.

$$|\Delta E| = c_0$$

For purposes of systems analysis, some ranges may elect to subdivide this error term into its individual error elements. In this case, the error equation may be represented as

$$c_0 = c_{\text{encoder bias}} + c_{\text{RF collimation bias}}$$

3.3.1.3 Measurement. In its strictest definition, elevation zero set is a measure of the difference between the encoder zero position and the perpendicular to the local gravity vector. The broader definition incorporates the difference produced by the RF axis collimation error along the elevation circle. The total static error is constant and is commonly determined by tracking a known truth standard (a satellite of known trajectory) and regressing the error from the trajectory solution.

3.3.2 Time Delay and Velocity Servo Lag. Velocity servo lag describes the situation in which the radar system is not pointing directly at a dynamically moving target being tracked. Because of the radar's inability to sufficiently adjust for a tracking error before, the angular velocity of the target creates a new tracking error. Time delay indicates an actual bias in the radar's timing, but the effect is identical to that of velocity servo lag.

3.3.2.1 Error Definition and Effects. As the radar system tracks a constant angular velocity target, the servo system responds to the displacement error and continually repositions the antenna to reduce the position error. A target moving with constant elevation velocity will require the antenna to rotate at a constant elevation velocity to overcome the position error. The constant error, caused by the constant angular velocity, remaining between the actual target position and the antenna position is called a velocity servo lag. Velocity servo lag is only significant for type 1 servo systems; this error is zero for type 2 systems.

3.3.2.2 Mathematical Form. The error constants, c_1 and c'_1 , have the units of time; therefore, multiplied by the elevation angular velocity, this error coefficient will yield the appropriate angular correction of

$$\begin{cases} \Delta E = c_1 \dot{E} & \text{Time Delay} \\ \Delta E = c'_1 \dot{E} & \text{Velocity Servo Lag} \end{cases}$$

In field procedures, the velocity servo lag measurement is commonly referred to as K_v . The relationship between c'_1 and K_v is $c'_1=1/K_v$.

3.3.2.3 Measurement. Measurement of the velocity servo lag value is radar specific and will not be addressed. Although the procedure performed in its entirety is lengthy and time consuming, many steps need not be repeated each time the velocity servo lag constant is determined. The system's K_v should be checked daily. This check takes approximately 15 minutes. If a truth standard (satellite of known trajectory) is available, the time delay (if any) may be estimated from the slope of a plot of the elevation residuals versus elevation rate.

3.3.3 Acceleration Servo Lag. Acceleration servo lag describes the situation in which the radar system is not pointing directly at a dynamically moving target being tracked. Because of the radar's inability to sufficiently adjust for a tracking error, the angular acceleration of the target creates a new tracking error.

3.3.3.1 Error Definition and Effects. As the radar system tracks a constantly accelerating target, the servo system must remain on track by continually overcoming the constantly changing velocity of the target. The acceleration constant is a measure of the radar system's ability to maintain track on the accelerating target and is related to the velocity constant. This value will change with each bandwidth setting.

3.3.3.2 Mathematical Form. The acceleration servo lag error constant, c_2 , has the units of time squared; therefore, multiplied by the elevation angular acceleration, this error coefficient will yield.

$$|\Delta E = c_2 \ddot{E}_e$$

In field procedures, the acceleration servo lag measurement is commonly referred to as K_a . The relationship between c_2 and K_a is $c_2=1/K_a$.

3.3.3.3 Measurement. Measurement of the acceleration servo lag value is radar specific and will not be addressed. Although the procedure performed in its entirety is lengthy and time consuming, many steps need not be repeated each time the acceleration servo lag constant is determined. The system's K_a can be determined and recorded on an operational basis only for the bandwidths which will be used during the operation. The K_a recordings can be made within a 20-30 minute period.

3.3.4 Pedestal Mislevel and Bearing Wobble (Azimuth Axis Roller Path). These terms account for the total amount of tilt of the azimuth axis in reference to the local vertical. This error is primarily caused by mounting irregularities and thermal gradients within the pedestal. In most cases, bearing wobble does not exist but rather is due to improper location of the levels.

3.3.4.1 Error Definition and Effects. Pedestal mislevel refers to the tilt of the azimuth axis from the local vertical. Azimuth axis rollerpath error (bearing wobble) is the result of imperfect azimuth axis bearings. Pedestal mislevel and azimuth axis rollerpath errors are discussed here together, because they have a similar effect on radar azimuth and elevation-angle error and both are measured in the same procedure. These errors are characterized by the first three harmonics of the cosine function. The first harmonic represents mislevel, while the remaining harmonic terms describe the azimuth axis rollerpath error. Of these, only the second harmonic is described in the error model. Mislevel error has a variable effect on the indicated-versus-true elevation parameter, depending upon the azimuth position of the pedestal. The error ranges between the peak-to-peak mislevel variation measured by the test; however, erroneous mislevel values will result from improperly installed equipment or faulty measurements.

3.3.4.2 Mathematical Form. In the mislevel and wobble equations below, c_3 and c_4 represent the desired coefficients of amplitude; β_1 and β_2 represent phase angle. A_1 is the measured azimuth corrected for zeroset and encoder nonlinearity.

$$\begin{array}{l} \Delta E = c_3 \cos (A_1 + \beta_1) \quad \text{Mislevel} \\ \Delta E = c_4 \cos (2A_1 + \beta_2) \quad \text{Wobble} \end{array}$$

3.3.4.3 Measurement. Mislevel is generally measured by mounting a level-reading device such as a Talyvel or inclinometer onto the radar pedestal and recording readings at uniform intervals throughout a 360° turn of the pedestal. These readings are then fit to a sinusoidal curve to determine amplitude and phase. Depending on resources, the interval may range from a maximum of 90° to a minimum of 0° (continuous). However, the gross motion of the pedestal precludes continuous measurements caused by vibration. Mislevel may also be determined by fitting a curve to the boresite measurements of several stars throughout a 360° turn.

3.3.5 Transit Time. This term accounts for the elevation error induced by the motion of the target as the reflected (or transmitted) radar pulse travels from the target at the finite speed of light. This error is typically only significant for great distances and velocities.

3.3.5.1 Error Definition and Effects. Transit-time errors arise because radar electromagnetic energy travels at a finite speed and cannot report the instantaneous position of the target. During a mission, the radar transmits a pulse which is then returned from the target either by beacon transmission or reflection. In the time that it takes for that return signal to travel back to the radar, the target will have moved a distance equal to the velocity of the target times the transit time of the signal. Consequently, at the time of completion of a radar measurement, the target has moved to a new position and a measurement error is present.

3.3.5.2 Mathematical Form. The transit-time equation derives from the assumption that elevation deltas and time intervals are sufficiently small to accurately approximate elevation rate. The estimated elevation velocity derives from the measured elevation value, and c_s represents the reciprocal of the speed of light as shown in

$$|\Delta E = c_s R_t \dot{E}_e$$

The use of the speed of light for trans-atmospheric purposes is a valid assumption, since the atmospheric effects are considered in the refraction error term. Correction of transit-time error can be achieved in one of two ways: by applying the foregoing equation to the measured data or by changing the time tag of the data.

3.3.5.3 Measurement. Since transit time is functionally related to the range and elevation rate values, the amount of error will vary throughout a mission. No fixed transit-time error can be measured and applied for a radar system. Accuracy is only affected by the selection of a speed of light standard which is accepted by the calibration community and the method by which \dot{E}_e is determined.

3.3.6 Encoder Nonlinearity. A precision shaft angle encoder is a device which translates the mechanical rotation of a shaft into an incremental electrical, digital representation. This term accounts for inaccuracies in the elevation data output resulting from deviations in the straight-line correlation of the input-shaft rotation and the incremental output electrical, digital representation caused by various factors such as environmental conditions, inherent-system errors, loading, and misalignment effects.

3.3.6.1 Error Definition and Effects⁴. The error produced is the difference between the encoder output and the actual elevation axis angular position resulting from misalignment in the mechanical linkage or manufacturing defects. The error is systematic and represents a nonlinear-functional change which

can be represented by an n-order harmonic series. For a direct drive encoder coupling, experience has indicated that measured nonlinearities for the first harmonic are very small and can usually be ignored. In most cases, the second harmonic is not related to the encoder but rather is induced by the operator during the test setup. The nonlinearity of the elevation encoder causes a variable bias to be introduced into the elevation-output data. Although the effect would be relatively small at close range, the magnitude of the error could become quite significant at long range.

The encoder coupling misalignment error has a complex relationship to the input angle. The three components considered are

- axial translation,
- radial translation from concentricity, and
- angle between rotational axes.

Each of these contributions to the coupling error is a function of the shaft angle position. These functions usually possess a periodicity equal to some submultiple of 360° but may have different average values and arbitrary phase relationships with respect to the input angles. Other error sources such as velocity, acceleration, and temperature exist but are not specifically addressed in this discussion. Some radars (FPS-16) may employ older systems where a coarse and fine encoder are used. Large errors in the 16th and 32d harmonics are commonly found in these systems.

3.3.6.2 Mathematical Form. The nonlinearity error effect causes a varying elevation angle output bias which follows the cosine of the elevation shaft angle change. The elevation zero-set and collimation-error measurements must be considered when encoder data is used for nonlinearity error determination purposes.

$$\begin{array}{l} \Delta E = c_6 \cos (n_1 E_o + \theta_1) \quad n_1 \text{ Harmonic} \\ \Delta E = c_7 \cos (n_2 E_o + \theta_2) \quad n_2 \text{ Harmonic} \\ \Delta E = c_8 \cos (n_3 E_o + \theta_3) \quad n_3 \text{ Harmonic} \end{array}$$

In the foregoing equation, c_6 , c_7 , and c_8 are the coefficients representing the amplitudes of the harmonic error, while θ_1 , θ_2 , and θ_3 represent the phase angles. The variables n_1 , n_2 , and n_3 indicate the harmonic number and are indicated here as representing the first three harmonics. In practice, they may represent any combination of harmonics.

3.3.6.3 Measurement⁴. The testing of a precision-angle encoder of any type should take into account all aspects of system performance as well as the interface between the encoder and the

system used. Measurement of the encoder nonlinearity is dependent upon the particular type and brand of encoding system. In general, the encoder output angle increment is compared against a precisely measured (via ULTRADEX or autocollimator) shaft angle increment through a turn of 180° in elevation. The recorded deviations of the encoder output from the true rotation are then modeled with the cosine series as discussed. The deviations will represent the summation of all contributing harmonics. As a result, caution must be exercised when attempting to model the function.

Static accuracy or resolution is a measure of the encoder's ability to correlate an infinitesimal rotation of the shaft with the transition from one encoder quantum state to another. Encoder resolution is equal to the number of quantized positions per turn of the input shaft. It contributes an uncertainty to the system output which is a fraction of the smallest quantum, known as the least significant bit (LSB) and is equal to one-half a quantum in the worst case. The quantum transition state is evidenced by the 'togglng' of the LSB from one number to the next and back again in a continuing rapid fluctuation.

3.3.7 Antenna Droop. This term accounts for the measured-elevation error induced by gravitational loading on the various components of the antenna assembly.

3.3.7.1 Error Definition and Effects. Because of a radar antenna's large mass, gravitational forces will act on it in sufficient measure to produce an elevation axis angle error that will depend on the moment arm presented to the gravity vector. Intuitively, the moment arm is a maximum at 0° elevation and a minimum at 90° elevation. The functional relationship of the error follows the cosine of the elevation angle. The antenna components most affected by droop are the reflector and feedhorn assembly and a cassegrain antenna subreflector.

3.3.7.2 Mathematical Form. From classical mechanics, it can be shown that the functional form of the droop effect is proportional to the cosine of the elevation angle. The coefficient, c_d , represents the maximum error value of droop (at 0° elevation), and E_1 assumes correction for zeroset and encoder nonlinearity.

$$|\Delta E = c_d \cos E_1$$

3.3.7.3 Measurement. The antenna-droop coefficient is generally a constant term which can be applied to real-time data as well as post-flight data. Measurement of droop is best achieved by modeling the functional form in a known trajectory which spans a wide range of elevation angles. Droop measurements using the boresite tower are theoretically possible, but experience has shown this method to be unacceptable for instrumentation radars.

3.3.8 Vertical Deflection. This term accounts for the azimuth difference induced by the misalignment of the local gravity vector from the normal vector of the ellipsoid reference model.

3.3.8.1 Error Definition and Effects. Strictly speaking, the deflection of the vertical is not an error in the radar measurement. Radar measurements must be made with respect to a coordinate system, and many radars use the astronomic vertical as an axis in their system. Radars that have their vertical axis aligned with the astronomic vertical make their measurements in an apparent or astronomic topocentric system referenced to the earth's geoid. While trajectory computations are most often performed on a mathematical ellipsoid such as DOD WGS-84, which closely approximates the size and shape of the geoid. The ellipsoid is a mathematically defined regular surface with specific dimensions. The geoid coincides with the surface to which the oceans would conform over the entire earth if free to adjust to the combined effect of the earth's mass attraction and the centrifugal force of the earth's rotation. As a result of the uneven distribution of the earth's mass, the geoidal surface is irregular. Since the ellipsoid is a regular surface, the two will not coincide. The areas of separation between the geoid and ellipsoid are referred to as geoid undulations, geoid heights, or geoid separations.

The geoid is a surface where the gravity potential is equal everywhere and where the gravity vector is always perpendicular. The angle between the perpendicular to the geoid (plumb line) and the perpendicular to the ellipsoid is defined as the deflection of the vertical. The vertical deflection angle is usually resolved into a north-south component which is coincident with the local meridian and equal to the difference between astronomic and geodetic latitude and an east-west component which is coincident with the prime vertical and proportional to the difference between astronomical and geodetic longitude. The north-south and east-west components of vertical deflection are referenced by the U.S. Geological Survey as ξ and η , with a north, south, east, or west identifier to indicate the direction in which the astronomic zenith is deflected relative to the geodetic zenith as viewed from a point in space. Thus, the correction for vertical deflection is really a coordinate system transformation from the astronomic topocentric to the geodetic topocentric coordinate system.

This transformation is determined by processing requirements and, in some cases, will lead to data degradation as a result of computer round off. Typically, this transformation is made because users of the radar data want it referenced to specific earth models such as WGS-84, or it will be combined with other instrumentation and the final trajectory estimate referenced to a specific earth model.

3.3.8.2 Mathematical Form. The equation describing vertical deflection uses the north-south and east-west components provided by the U.S. Geological Survey. The following equation provides the elevation error as a function of azimuth; there are no coefficients to be determined. A_2 is the adjusted azimuth angle of measurement.

$$|\Delta E = \eta \sin A_2 + \xi \cos A_2$$

Confusion with the polarity of the variables of vertical deflection generally arises from the local sign convention. A review of local procedures is warranted to ensure proper use of this error term, particularly in regions of the world where vertical deflection is significantly large.

3.3.8.3 Measurement. Although measurement by each range is possible, it is generally better to use the values provided by the Defense Mapping Agency.

3.3.9 Refraction and Residual Refraction. This term accounts for the errors induced in the elevation measurement by an inappropriate or inaccurate refraction model correction.

3.3.9.1 Error Definition and Effects. Elevation refraction errors are the result of refractive index changes caused by bending the propagation path of electromagnetic energy. In a typical atmosphere, the refractive gradient will decrease smoothly with increasing height; however, anomalies will exist for various reasons and result in an inaccurate representation of the atmospheric characteristics.

3.3.9.2 Mathematical Form. Although presented as a constant, this variable could actually represent any number of functions designed to specifically address shortcomings in the refraction model applied to the data. The danger of such an open-ended approach is that it may actually absorb errors attributable to other systematic error sources during a regression analysis routine, depending on the functional form this variable takes.

$$\begin{array}{l} |\Delta E = \rho_E \quad \text{Refraction} \\ |\Delta E = \rho'_E \quad \text{Residual Refraction} \end{array}$$

3.3.9.3 Measurement. Refraction errors are determined through the use of sophisticated mathematical models based on inputs from the local environment. Residual refraction is intended to address errors associated with inaccurate weather condition inputs to the refraction model.

3.4 DOPPLER RANGE RATE COMPONENT

3.4.1 Transit Time. This term accounts for the range rate error induced by the motion of the target as the reflected (or transmitted) radar pulse travels from the target at the finite speed of light. This error is typically only significant for great distances and velocities.

3.4.1.1 Error Definition and Effects. Transit-time errors arise because radar electromagnetic energy travels at a finite speed and cannot report the instantaneous position of the target. During a mission, the radar transmits a pulse which is then returned from the target either by beacon transmission or reflection. In the time that it takes for that return signal to travel back to the radar, the target will have moved a distance equal to the velocity of the target times the transit time of the signal. If that movement has resulted in a corresponding change in range rate, then at the completion of a radar measurement, a measurement error is present.

3.4.1.2 Mathematical Form. In the transit time equation, range rate deltas and time intervals are sufficiently small to accurately approximate the first derivative of the range rate. The estimated range acceleration is derived from the measured range rate value, while d_1 represents the reciprocal of the speed of light.

$$|\Delta RR = d_1 R_1 \ddot{R}_e$$

The use of the vacuum speed of light for trans-atmospheric purposes is a valid assumption, since the atmospheric effects are considered in the refraction error term. Correction of transit-time error can be achieved in one of two ways: by applying the foregoing equation to the measured data or by changing the time tag of the data.

3.4.1.3 Measurement. Since transit time is functionally related to the range and acceleration values, the amount of error will vary throughout a mission. There is no fixed transit-time error which can be measured and applied for a radar system. Accuracy is only affected by the selection of a speed of light standard which is accepted by the calibration community and the method by which \ddot{R}_e is determined.

3.4.2 Time Delay and Acceleration Servo Lag. Acceleration servo lag for Doppler range rate describes an error condition not applicable to most modern radar systems. Time delay reflects an actual bias in the radar's timing which is identical in its effect on the range rate measurement to acceleration servo lag.

3.4.2.1 Error Definition and Effects. Doppler range rate is determined by measuring the shift between the transmitted and received frequencies during tracking as determined by the local oscillator. In practice, some systems measure the pulse-to-pulse rate signal phase change, but in either case, the radial velocity of a target is determined by exploiting the Doppler effect. If a track has been established long enough to remove initial transients, a target moving with constant velocity (radial) can be tracked with minimal error. If the target is accelerating (radially) at a constant rate, then there will be a lag in radar's ability to follow the instantaneous velocity. This error is known as acceleration servo lag. In most systems equipped for Doppler tracking, this term is considered insignificant because of a tight tracking loop.

3.4.2.2 Mathematical Form. If applicable, this equation will account for acceleration servo lag and time delay effects. If not applicable, d_2 and d'_2 may be set to zero in the radar error model equation.

$$\begin{cases} \Delta RR = d_2 \ddot{R}_r & \text{Time Delay} \\ \Delta RR = d'_2 \ddot{R}_r & \text{Acceleration Servo Lag} \end{cases}$$

3.4.2.3 Measurement. Measurement of the acceleration servo lag is radar specific and will not be addressed. Time delay is also a radar (or range) specific error condition and should be determined according to applicable procedures.

3.4.3 Jerk Servo Lag. Jerk servo lag describes an error condition not applicable to most modern radar systems.

3.4.3.1 Error Definition and Effects. Doppler range rate is determined by measuring the shift between the transmitted and received frequencies during tracking as determined by the local oscillator. In practice, some systems measure the pulse-to-pulse rate signal phase change, but in either case, the radial velocity of a target is determined by exploiting the Doppler effect. If a track has been established long enough to remove initial transients, a target moving with constant acceleration (radial) can be tracked with minimal error. If the acceleration (radial) changes, then there will be a lag in radar's ability to follow the instantaneous acceleration. This error is known as jerk servo lag, and in most systems equipped for Doppler tracking, this term is considered insignificant because of a tight tracking loop.

3.4.3.2 Mathematical Form. If applicable, this equation will account for jerk servo lag. If not applicable, d_3 may be set to zero in the radar error model equation.

$$\Delta RR = d_3 \dddot{R}_r$$

3.4.3.3 Measurement. Measurement of the jerk servo lag is radar specific and will not be addressed.

3.4.4 Refraction and Residual Refraction. This term accounts for errors induced into the range-rate measurement by an inappropriate or inaccurate refraction model correction.

3.4.4.1 Error Definition and Effects. Range-rate refraction errors are caused by variations in the propagation velocity of the radar's electromagnetic energy which yield an incorrect range-rate measurement. Residual refraction errors result from an incorrect assessment or estimate of the refractive index of the atmosphere along the signal path. The ability to properly assess the conditions is limited by the discrete number of observations made, the timeliness of the data, and refractive anomalies along the propagation path.

3.4.4.2 Mathematical Form. Although presented as a constant, these variables could actually represent any number of functions designed to specifically address refraction of the data.

$$\left| \begin{array}{l} \Delta R = \rho_{RR} \quad \text{Refraction} \\ \Delta R = \rho'_{RR} \quad \text{Residual Refraction} \end{array} \right.$$

3.4.4.3 Measurement. Refraction for Doppler range-rate measurements is calculated by taking the first derivative with respect to time of the range refraction calculated for range. Residual refraction is the first derivative of the residual refraction for range.

CHAPTER 4

RADAR SYSTEMATIC ERROR MODEL DERIVATION

Chapter 4 provides a derivation for each of the error-model terms described in chapter 3. In this chapter, the discussion does not follow a one-to-one correspondence with those terms in the preceding chapters. Rather, the components (range, azimuth, elevation, and doppler) of several error terms have been combined under one discussion in cases where the derivation proceeds from a common point or assumption (see paragraph 4.1). The derivation of the refraction term is complex and is left to a separate discussion (see paragraph 4.2).

For the purpose of this derivation, error is defined as the difference between the measurement (or computed) value and the true value. The true value is, of course, unknowable; however, for practical applications it comes from some standard that is sufficiently more accurate than the system being calibrated. The total error is the resultant sum of all systematic error terms.

4.1 RADAR SYSTEM ERRORS

4.1.1 Static Errors. The static error or bias is characterized by a constant offset from the true value. Sources of this error can be many including encoder zero-set, range-beacon delay, and operator alignment. As for the error model, the equations for range, azimuth, and elevation are simply

$$\Delta R = \text{constant}_R$$

$$\Delta A = \text{constant}_A$$

$$\Delta E = \text{constant}_E$$

4.1.2 Servo Lag⁴. There are two types of feedback control systems commonly found in monopulse radars:

Type 1: Zero-displacement-error system. A constant reference input signal will produce a constant velocity of the controlled output.

Type 2: Zero-velocity-error system. A constant reference input signal will produce a constant acceleration of the controlled output.

The equation which relates the response or output function to the input function is

$$\psi_o(t) = \psi(t) - \varepsilon(t)$$

where

$$\begin{aligned}\psi_o(t) &= \text{output function} \\ \psi(t) &= \text{input function} \\ \varepsilon(t) &= \text{error function}\end{aligned}$$

Servo lag corrections deal with steady state error. A type 1 system can follow a constant velocity input with zero velocity error but with a constant displacement error. This displacement error is due to a lag in the servo's ability to develop the required velocity, and is given by

$$\varepsilon = \dot{\psi} / K_v$$

where $\dot{\psi}$ is the constant-velocity input and K_v is the servo's velocity error constant. For a zero-velocity input, there is zero-displacement error.

A type 2 system can do better; it can follow a constant-acceleration input with zero velocity and acceleration errors. Under constant velocity (zero acceleration) input, it is able to zero out the displacement error encountered with a type 1 system. Under a constant, nonzero acceleration input, however, a type 2 system also produces a displacement error caused by servo lag. This error is given by

$$\varepsilon = \ddot{\psi} / K_a$$

where $\ddot{\psi}$ is the constant acceleration input and K_a is the servo's acceleration-error constant. Note that for a constant velocity (zero acceleration) input there is zero-displacement error.

Software can correct for these steady-state errors by using calculated values for velocity and acceleration and input values of K_v or K_a . (Actually, values for $1/K_v$ and $1/K_a$ are generally used as input.) Errors are calculated separately for the range, azimuth, and elevation channels.

$$\Delta R = (1/K_v^R) \dot{R} \text{ or } (1/K_a^R) \ddot{R}$$

$$\Delta A = (1/K_v^A) \dot{A} \text{ or } (1/K_a^A) \ddot{A}$$

$$\Delta E = (1/K_v^E) \dot{E} \text{ or } (1/K_a^E) \ddot{E}$$

where the K_v or K_a represent the appropriate servo-error constants for range, azimuth, or elevation.

4.1.3 Pedestal Mismatch⁴. Figure 4-1 shows the azimuth circle in the horizontal plane and a mismatch plane. The platform (or pedestal) has been misaligned with respect to the horizontal.

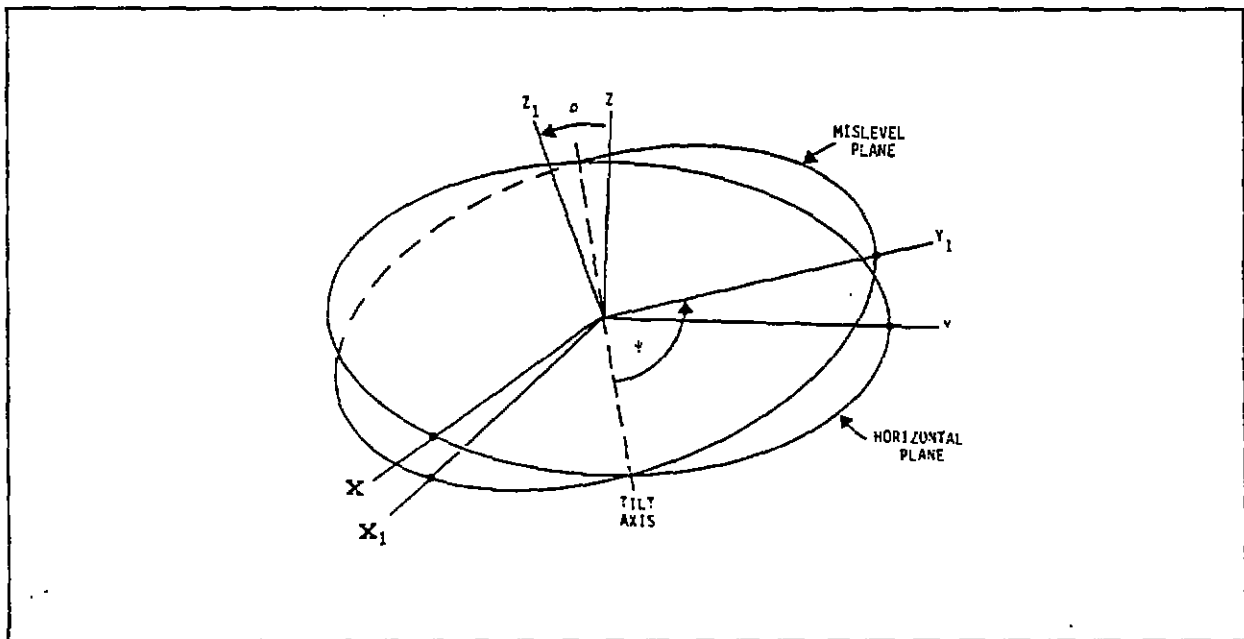


Figure 4-1. Mislevel geometry.

The following rotation will align the X_1, Y_1, Z_1 system with the XYZ system

$$\begin{bmatrix} X \\ Y \\ Z \end{bmatrix} = R_{Z_1}(-\psi) R_{Y_1}(\rho) R_{Z_1}(\psi) \begin{bmatrix} X_1 \\ Y_1 \\ Z_1 \end{bmatrix} \quad (4-1)$$

where

$$R_{Z_1}(\psi) = \begin{bmatrix} \cos\psi & \sin\psi & 0 \\ -\sin\psi & \cos\psi & 0 \\ 0 & 0 & 1 \end{bmatrix}$$

$$R_{Y_1}(\rho) = \begin{bmatrix} 1 & 0 & -\rho \\ 0 & 1 & 0 \\ \rho & 0 & 1 \end{bmatrix}$$

$$R_{Z_1}(-\psi) = \begin{bmatrix} \cos\psi & -\sin\psi & 0 \\ \sin\psi & \cos\psi & 0 \\ 0 & 0 & 1 \end{bmatrix}$$

Then equation 4-1 becomes

$$\begin{bmatrix} X \\ Y \\ Z \end{bmatrix} = \begin{bmatrix} X_1 - \rho Z_1 \cos\psi \\ Y_1 - \rho Z_1 \sin\psi \\ X_1 \rho \cos\psi + Y_1 \rho \sin\psi + Z_1 \end{bmatrix}$$

and

$$\Delta X = -\rho Z_1 \cos\psi$$

$$\Delta Y = -\rho Z_1 \sin\psi$$

$$\Delta Z = X_1 \rho \cos\psi + Y_1 \rho \sin\psi$$

These errors must now be transformed into ΔR , ΔA , and ΔE by

$$R = \sqrt{X^2 + Y^2 + Z^2}$$

$$A = \tan^{-1}(X / Y)$$

$$E = \tan^{-1} \left[\frac{Z}{\sqrt{X^2 + Y^2}} \right]$$

The first order differences are

$$\Delta R = 0$$

$$\Delta A = (\partial A / \partial X) \Delta X + (\partial A / \partial Y) \Delta Y$$

$$\Delta E = (\partial E / \partial X) \Delta X + (\partial E / \partial Y) \Delta Y + (\partial E / \partial Z) \Delta Z$$

Then, by substitution,

$$\Delta A = \rho \sin(A + \phi) \tan E$$

$$\Delta E = \rho \cos(A + \phi)$$

where

$$\phi = \pi/2 - \psi.$$

4.1.4 Electrical Misalignment (Collimation)⁴. The electrical axis and the mechanical axis can be misaligned. There are two directions to this misalignment: one along the elevation circle and the other perpendicular to the plane of the elevation circle. Figure 4-2 shows this relationship.

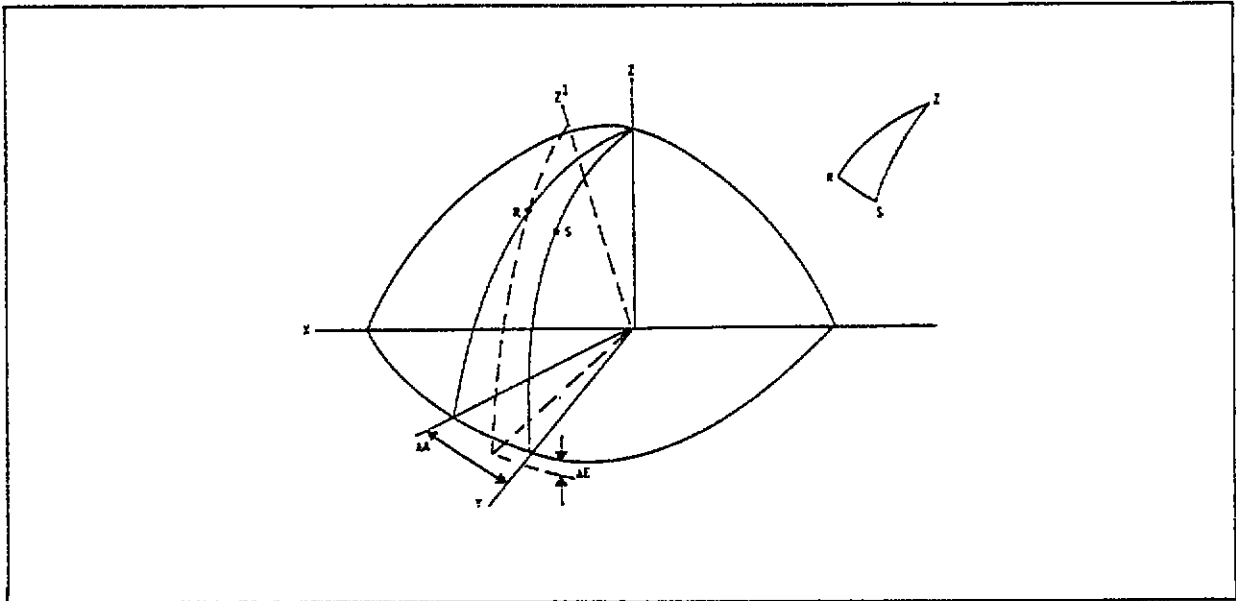


Figure 4-2. Electrical misalignment geometry.

From figure 4-2 and the principles of spherical trigonometry, the errors are given as

$$\tan(\Delta A) = \frac{\tan(A_M)}{\cos(E)} \approx \Delta A$$

or

$$\Delta A = A_M \sec E$$

and

$$\Delta E = E_M$$

which is constant and absorbed in the elevation zero set, E_0 .

4.1.5 Nonorthogonality (Standards)⁴. The term "standards" is also given to nonorthogonality, because the elevation axis is supported by the standards. If the standards are not the same height, the elevation axis will not be orthogonal to the azimuth axis. See figure 4-3 for an illustration.

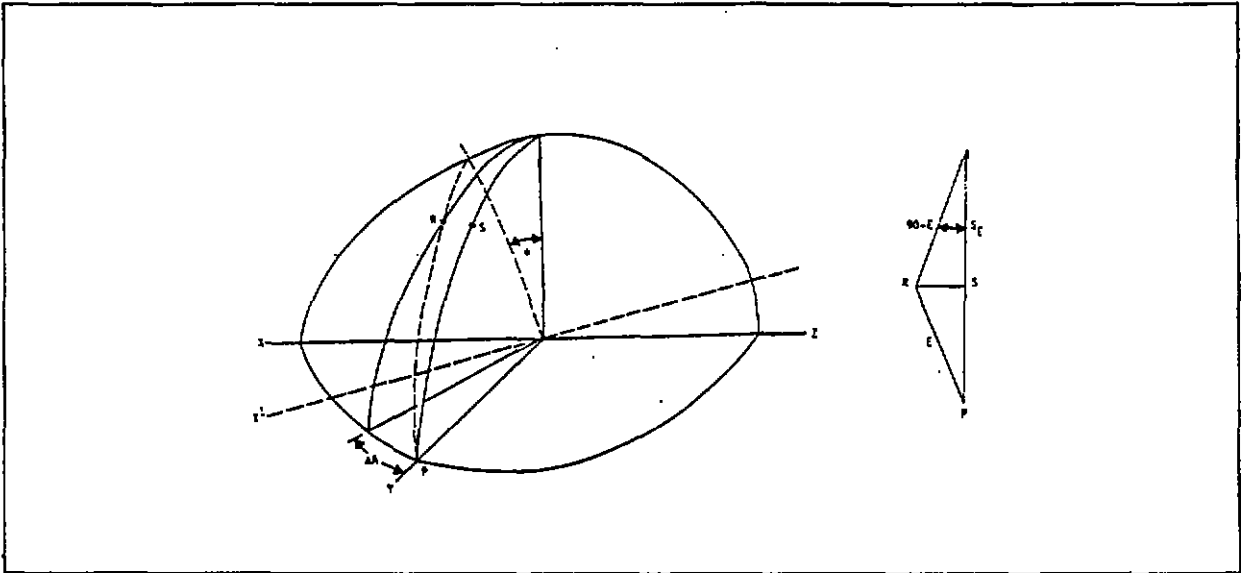


Figure 4-3. Nonorthogonality geometry.

From figure 4-3 and the principles of spherical trigonometry, the following relationships are found to exist:

$$\tan(RS) = \tan(\phi) \sin(E)$$

$$\tan(RS) = \tan(S_E) \cos(E)$$

or by rearranging,

$$\tan(S_E) = \tan(\phi) \tan(E)$$

Now, let

$$K = \tan \phi$$

and for small angles, $S_E = \tan S_E$. Substituting gives

$$S_E = K \tan E$$

$$\Delta A = K \tan E$$

$$\Delta E \approx 0$$

4.1.6 Encoder Nonlinearity⁴. Encoder nonlinearity is primarily due to the construction of the encoder itself. The encoder measures an angle based on the encoder's mechanical axis. When the encoder is coupled to an azimuth or elevation shaft, perfect mechanical alignment of the mechanical axis of the shaft and encoder is not possible. The problem is compounded when the angle measuring device is a multiple stage system such as a resolver. Figure 4-4 shows the situation.

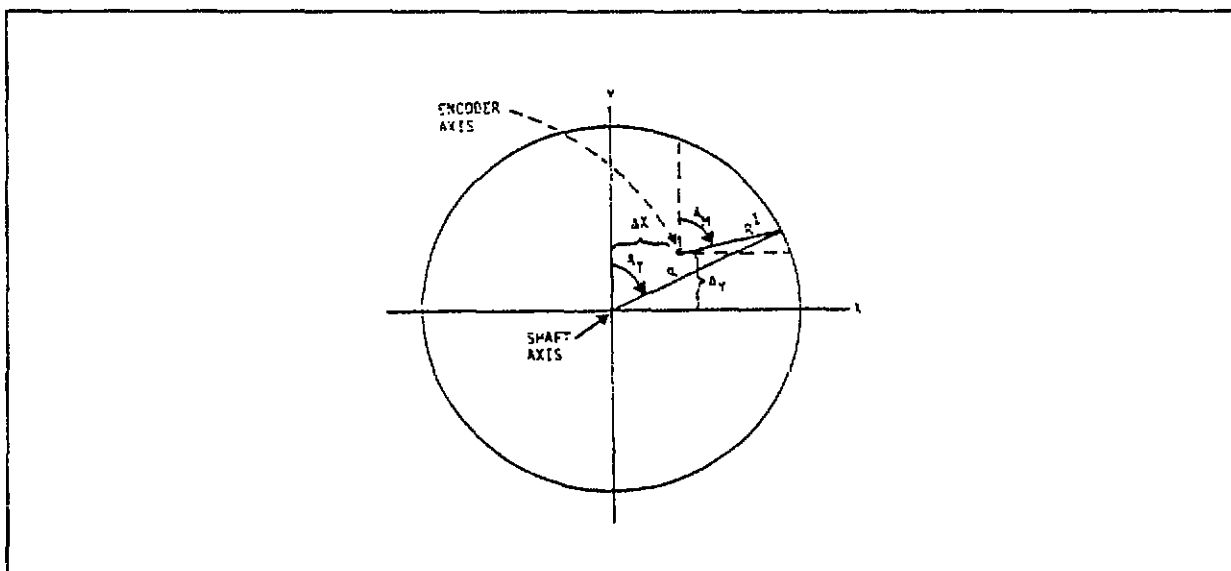


Figure 4-4. Encoder nonlinearity geometry.

From figure 4-4,

$$X = R \sin A_T \text{ and } Y = R \cos A_T$$

$$R^2 = X^2 + Y^2 \text{ and } A_T = \tan^{-1}(X/Y)$$

Linearizing gives

$$\Delta A_T = (\partial A_T / \partial X) \Delta X + (\partial A_T / \partial Y) \Delta Y$$

$$= (Y/R^2) \Delta X - (X/R^2) \Delta Y$$

$$= (Y/R) \cdot (\Delta X/R) - (X/R) \cdot (\Delta Y/R)$$

Then, by substitution

$$\Delta A = (\Delta X / R) \cos A - (\Delta Y / R) \sin A$$

or

$$\Delta A = A_N \sin A + B_N \cos A$$

The X-Y coordinate system can be defined so that $\Delta X = \Delta Y$; then, the error equations become

$$\Delta A = A_N \cos (A + \phi)$$

$$\Delta E = E_N \cos (E + \phi)$$

4.1.7 Antenna Droop⁶. Because of a radar antenna's large mass, gravity will act on it to produce a deflection (droop) in the elevation that will depend on the moment arm presented to the gravity vector. Intuitively, the moment arm is maximum at 0° elevation and zero at 90° elevation. Figure 4-5 shows this relationship.

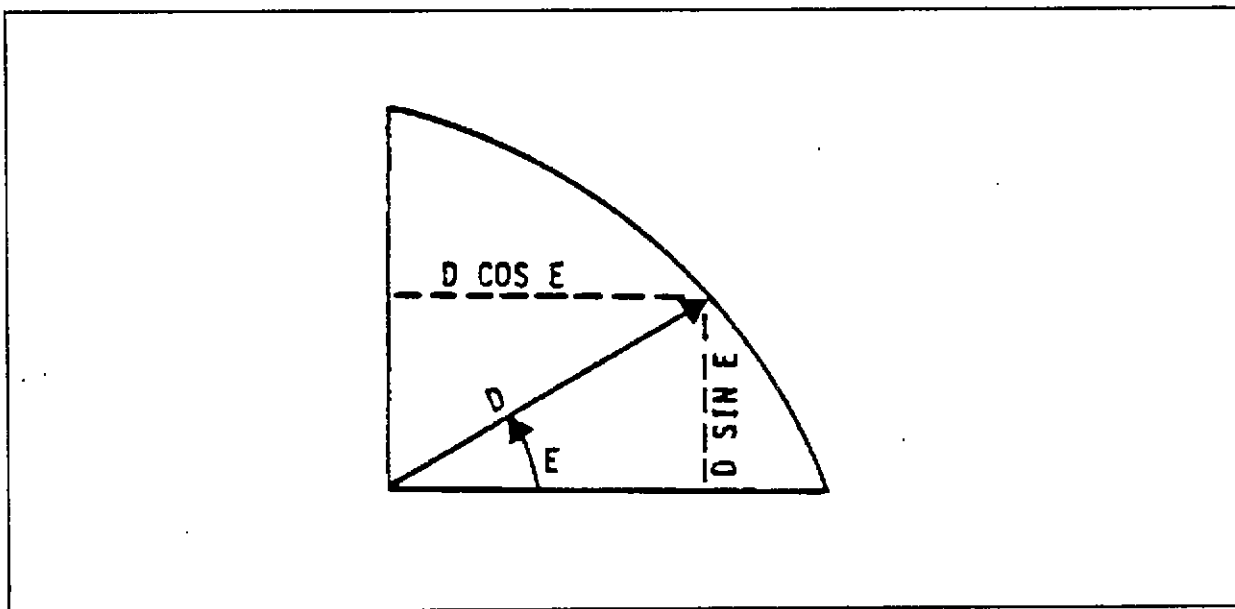


Figure 4-5. Droop geometry.

The derivation of droop can be simplified by thinking of the antenna assembly as a solid beam with the entire mass of the antenna assembly concentrated at a distance D from the center of rotation of the elevation system. It can be further assumed that no bending of the beam occurs. From classical mechanics, the deflection at the end of the beam at a distance $x=D\cos E$ is given by the following equation:

$$y = -x \frac{W}{2nA}$$

The mass of the antenna is acted upon by gravity in a downward direction only to produce a force which creates the deflection y. W constitutes this force, n is the shear modulus, and A is the cross-sectional area of the beam. The negative sign indicates the deflection to be downward.

Substituting a constant, K, which is equal to $-W/2nA$, the equation becomes

$$\Delta E = y = KD\cos E$$

The product KD is the droop coefficient, c_9 , in the error model description.

4.1.8 Vertical Deflection^{7,8}. Vertical deflection results from the fact that in geodesy the irregular shape of the earth is approximated by a mathematical surface. The irregular shape is known as the geoid and represents the gravimetric equal potential surface. The geoid coincides with the surface to which the ocean would conform over the entire earth if free to adjust to the combined effects of the earth's mass attraction and the centrifugal forces of the earth's rotation. The mathematical surface is an ellipsoid of rotation that "best fits" the shape of the geoid. Vertical deflection results from the fact that the normals to these two surfaces are not coincident (see figure 4-6).

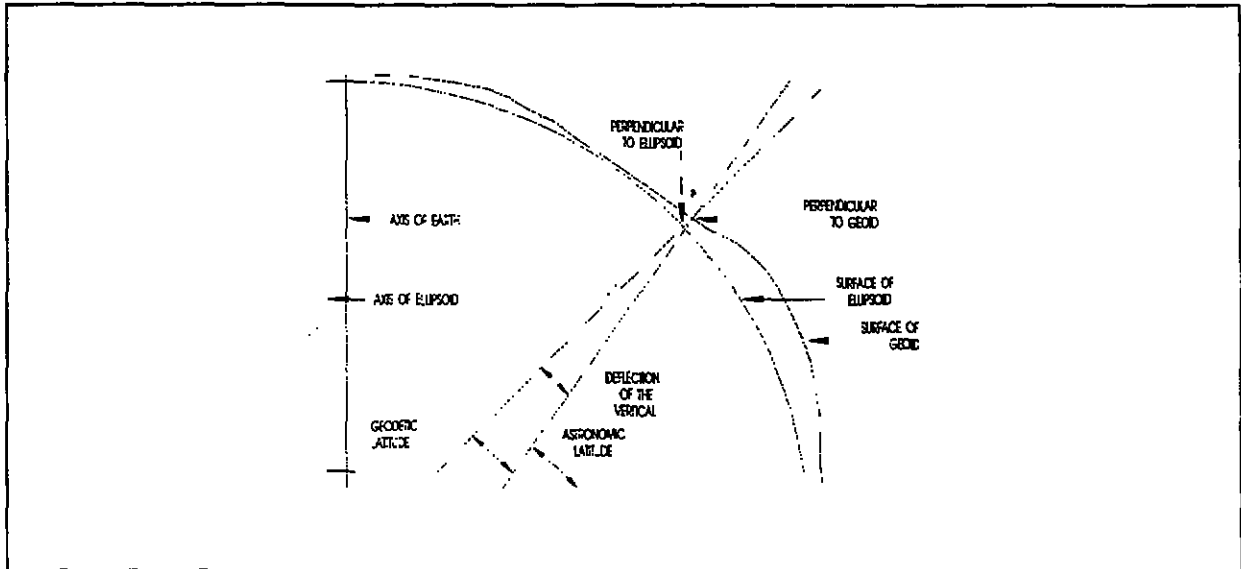


Figure 4-6. Vertical deflection.

Consider a point P near the surface of the earth (see figure 4-6). From point P a geodetic vertical may be erected which is normal to the mathematical surface of the ellipsoid. A vertical may also be erected which is normal to the irregular surface of the geoid at P. This vertical would be that of a plumb line. The angular separation of these two vertical lines is called the vertical deflection. As can be seen in figure 4-6 these two verticals have different latitudes and longitudes. The vertical referenced to the geoid is called the astronomic vertical and has the corresponding astronomic latitude and longitude. The vertical referenced to the ellipsoid is called the geodetic vertical and has corresponding geodetic latitude and longitude.

The deflection of the vertical at an instrument site, say point P, is defined by

$$\xi = (\phi_A - \phi) \quad \text{the deviation in the meridian}$$

$$\beta = (\lambda_A - \lambda) \quad \text{the deviation in longitude}$$

$$\eta = \beta \cos \phi \quad \text{the deviation in the prime vertical}$$

Two rectangular coordinate systems with coincident origins both at P establish the astronomic and geodetic local level rectangular coordinate systems. For convention, let X be positive east, Y be positive north, and Z be the particular vertical in question. Then the transformation from one system to the other system is accomplished by the three axis rotation:

$$\begin{bmatrix} X_G \\ Y_G \\ Z_G \end{bmatrix} = \begin{bmatrix} l_1 & m_1 & n_1 \\ l_2 & m_2 & n_2 \\ l_3 & m_3 & n_3 \end{bmatrix} \begin{bmatrix} X_A \\ Y_A \\ Z_A \end{bmatrix}$$

where the row subscripted with a 1 contains the direction cosines of the X_G axis in the astronomic system, the row subscripted with a 2 contains the direction cosines of the Y_G axis in the astronomic system, and the row subscripted with a 3 contains the direction cosines of the Z_G axis in the astronomic system. Using the exact definitions of these direction cosines, a rotation matrix can be defined as

$$M = \begin{bmatrix} \cos\beta & -\sin\phi_A \sin\beta & \cos\phi_A \sin\beta \\ \sin\phi \sin\beta & \cos\xi - \sin\phi_A \sin\phi (1 - \cos\beta) & \sin\xi + \sin\phi \cos\phi_A (1 - \cos\beta) \\ -\cos\phi \sin\beta & -\sin\xi + \sin\phi_A \cos\phi (1 - \cos\beta) & \cos\xi - \cos\phi_A \cos\phi (1 - \cos\beta) \end{bmatrix}$$

Then, the following relations are exact transformations between astronomic system and geodetic system:

$$\begin{bmatrix} X \\ Y \\ Z \end{bmatrix}_G = M \begin{bmatrix} X \\ Y \\ Z \end{bmatrix}_A$$

and

$$\begin{bmatrix} X \\ Y \\ Z \end{bmatrix}_A = M^T \begin{bmatrix} X \\ Y \\ Z \end{bmatrix}_G$$

The typical radar coordinates, (R)ange, (A)zimuth, and (E)levation are related to the Cartesian coordinates X, Y, and Z as follows:

$$\begin{aligned} X &= R \cos(E) \sin(A) \\ Y &= R \cos(E) \cos(A) \\ Z &= R \sin(E) \end{aligned}$$

and

$$R = \sqrt{X^2 + Y^2 + Z^2}$$

$$A = \tan^{-1} \frac{X}{Y}$$

$$E = \tan^{-1} \frac{Z}{\sqrt{X^2 + Y^2}}$$

The steps in transforming radar data from one system to the other system involve first transforming range, azimuth, and elevation to X, Y, and Z; making the appropriate rotation; and then transforming the rotated X, Y, and Z back to range, azimuth, and elevation.

By making small angle assumptions, a first-order approximation for the rotation matrix would be

$$\begin{bmatrix} 1 & -\eta \tan \phi & \eta \\ \eta \tan \phi & 1 & \xi \\ -\eta & -\xi & 1 \end{bmatrix}$$

where ϕ is either the astronomic or geodetic latitude without further impairment of accuracy. Having made these assumptions,

$$\Delta A = A_A - A_G = \eta \tan \phi - \eta \tan E \cos A + \xi \tan E \sin A$$

$$\Delta E = E_A - E_G = \eta \sin A + \xi \cos A$$

4.2 ATMOSPHERIC ERRORS

4.2.1 Refraction Technical Description. Because of the many refractive layers of atmosphere through which an electromagnetic wave must travel, the refraction problem is complex. The refraction routines discussed next were developed for the Eastern Test Range by Mr. Gerald Trimble.⁹ Actually, two options exist for refraction corrections:

- Option 1 - REEK, a completely rigorous ray-trace method which solves the differential equation of a ray traveling through a spherically stratified atmosphere.
- Option 2 - TRFR, a fast approximation to the refraction corrections provided by REEK (within 3 percent). The TRFR uses REEK to build a table of refraction profiles prior to processing any data. Since TRFR is a subset of REEK, this option will not be discussed.

4.2.1.1 REEK Refraction⁹. The subroutine REEK is designed to compute range and elevation refraction corrections in the troposphere and ionosphere for both pulse (group) or continuous wave (phase) systems. There are no practical limitations on range or elevation values. The atmosphere characteristics may be supplied as an explicit profile of refractivity versus height or in terms of some reference profile plus a ground index to correct for local moisture conditions. Two different types of data input may be presented to REEK: observed and true.

Observed input of range (R) and elevation angle (ϕ_0) implies that the instrument is looking along that elevation angle (ϕ_0) and the return pulse is sensed $2R/C$ seconds after it is emitted. The curved path is $(R - \epsilon_R)$ long where ϵ_R is the retardation refraction correction (see figure 4-7).

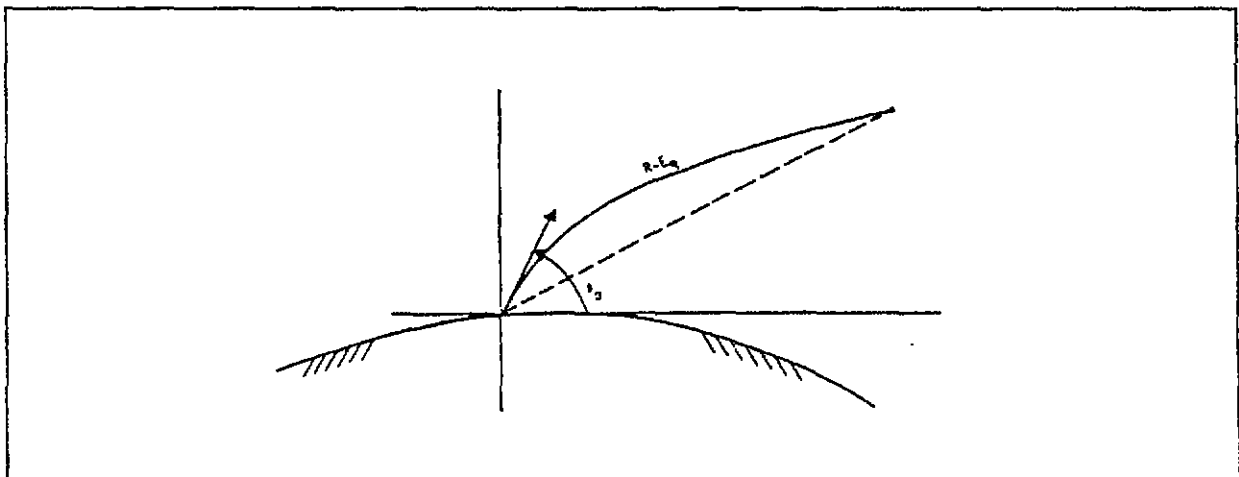


Figure 4-7. Geometry of observed input.

True input of range (R) and elevation (ϕ_0) implies that the instrument sees an object located on a straight line of elevation angle ϕ_0 and range R (see figure 4-8).

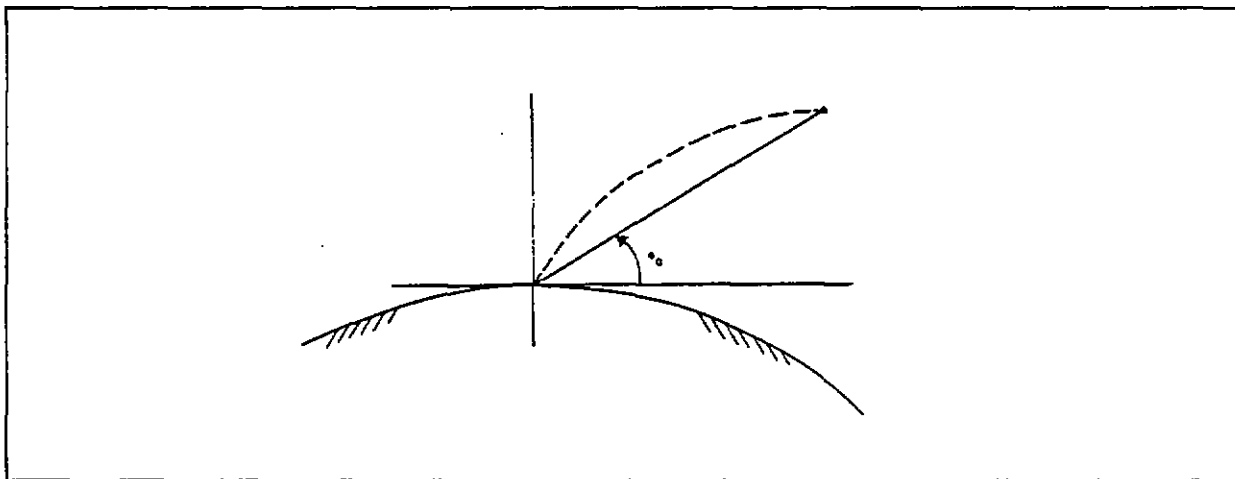


Figure 4-8. Geometry of true input.

The retardation correction is the speed difference between a ray traveling in a refractive medium and a ray traveling in a vacuum. In the troposphere, the phase refractivity values (n) are greater than 1 and profile values, which are in terms of $n-1$, are positive. Also, no difference exists between group and phase corrections. In the ionosphere, the phase refractivity is less than 1, and the profile terms are negative. Additionally, considerable differences exist between group and phase retardation corrections.

4.2.1.2 Differential Equation of a Ray (Spherically Stratified Case). The velocity of an electromagnetic wave in a refractive medium is

$$v = \frac{ds}{dt} = \frac{C}{n} \quad (4-2)$$

where

- s = distance along the path
- C = wave propagation speed in a vacuum
- n = phase refractivity

The components of equation 4-2 expressed in a two-dimensional polar coordinate system are

$$\frac{d\Theta}{dt} = \frac{C}{n} \cdot \frac{\cos\phi}{(R_e + h)} \quad (4-3)$$

$$\frac{dh}{dt} = \frac{C}{n} \cdot \sin\phi \quad (4-4)$$

where

Θ = geocentric angle from site

h = height above the earth

ϕ = angular direction of the ray relative to local horizontal

R_e = radius of earth (assumed spherical)

(See figure 4-9).

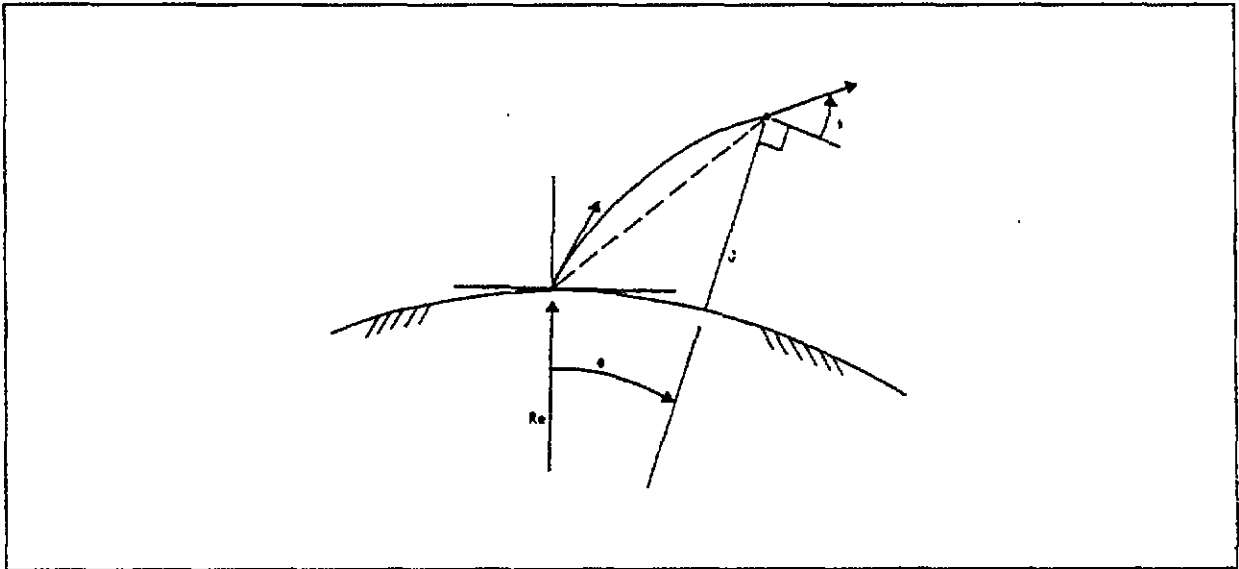


Figure 4-9. Definition of terms.

From equation 4-2,

$$dt = \frac{n}{C} ds$$

so that equations 4-3 and 4-4 become

$$\frac{d\Theta}{ds} = \frac{\cos\phi}{(R_e+h)} \quad (4-5)$$

$$\frac{dh}{ds} = \sin\phi \quad (4-6)$$

A vector K which describes the three-dimensional ray-path curvature in a refractive medium is

$$K = \frac{1}{n} (\hat{I}_T \times \nabla n) \quad (4-7)$$

where

\hat{I}_T = ray tangent unit vector
 ∇n = refractivity gradient
 n = local refractivity scalar

The initial three-dimensional ray-tangent vector, assuming for convenience that it lies in the (Θ, R) plane, is

$$I = \hat{I}_\Theta \left(R \frac{d\Theta}{ds} \right) + \hat{I}_R \left(\frac{dR}{ds} \right) + \hat{I}_a(0) \quad (4-8)$$

Substituting equations 4-5 and 4-6 into 4-8, and noting that

$$\frac{dR}{ds} = \frac{dh}{ds}$$

gives

$$\hat{I}_T = \hat{I}_\Theta (\cos\phi) + \hat{I}_R (\sin\phi) + \hat{I}_a(0)$$

where

\hat{I}_a = unit vector normal to R and \hat{I}_T
 \hat{I}_R = unit vector along R
 \hat{I}_Θ = unit vector normal to \hat{I}_a and \hat{I}_R
 R = position vector from earth center

Based on the assumption of a spherically stratified atmosphere, the refractivity gradient is

$$\nabla n = \hat{I}_\Theta(0) + \hat{I}_R \left(\frac{\partial n}{\partial R} \right) + \hat{I}_a(0)$$

or since

$$\frac{\partial n}{\partial R} = \frac{\partial n}{\partial h}$$

$$\nabla n = \hat{i}_\Theta(0) + \hat{i}_R \left(\frac{\partial n}{\partial h} \right) + \hat{i}_a(0)$$

Combining these results, equation 4-7 becomes

$$K = \frac{1}{n} \left[\hat{i}_\Theta(0) + \hat{i}_R(0) + \hat{i}_a \left(\cos \phi \frac{\partial n}{\partial h} \right) \right]$$

which implies that the ray path remains in the (Θ, R) plane, and hence, the a component remains zero length.

If δ is the path angle in the (Θ, R) plane, referenced to the initial horizontal, then $d\delta/ds$ defines the signed curvature magnitude,

$$\frac{d\delta}{ds} = \pm |K| = \frac{1}{n} \cos \phi \frac{dn}{dh} \quad (4-9)$$

Then from figure 4-10, the following relationships are true:

$$\frac{d\phi}{ds} = \frac{d\delta}{ds} + \frac{d\Theta}{ds}$$

and

$$\phi = \delta + \Theta$$

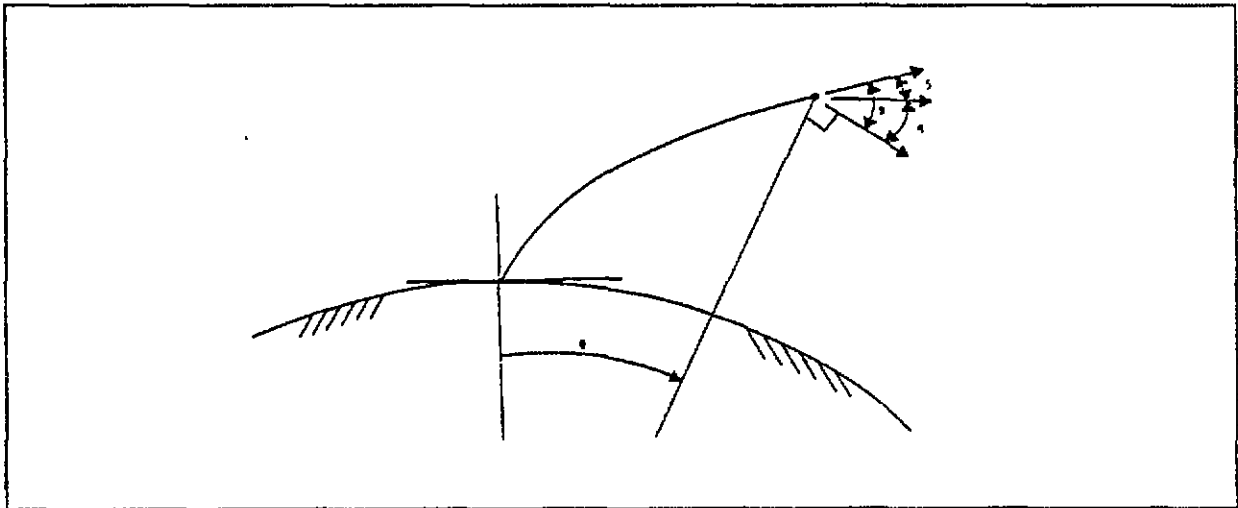


Figure 4-10. Relationship for bending.

The basic differential equations of the ray are 4-5, 4-6 and 4-9, assuming spherical stratification of the atmosphere.

4.2.1.3 Range and Elevation Refraction Correction. An additional differential equation is derived which will accumulate only the range refraction corrections as a ray-trace solution of the previous differential equations proceed. Accumulating range corrections separately is done in the interest of accuracy because of the large numbers associated with range. The derivation individually includes both the bending portion and the retardation portion of the range correction.

4.2.1.3.1 Range Bending Correction. The range bending correction (ϵ_b) is defined as the difference in the length of the actual ray path traversed (S) and the straight line (R) connecting the end points of the ray. ϵ_b is expressed as

$$\epsilon_b = S - R \quad (4-10)$$

(See figure 4-11.)

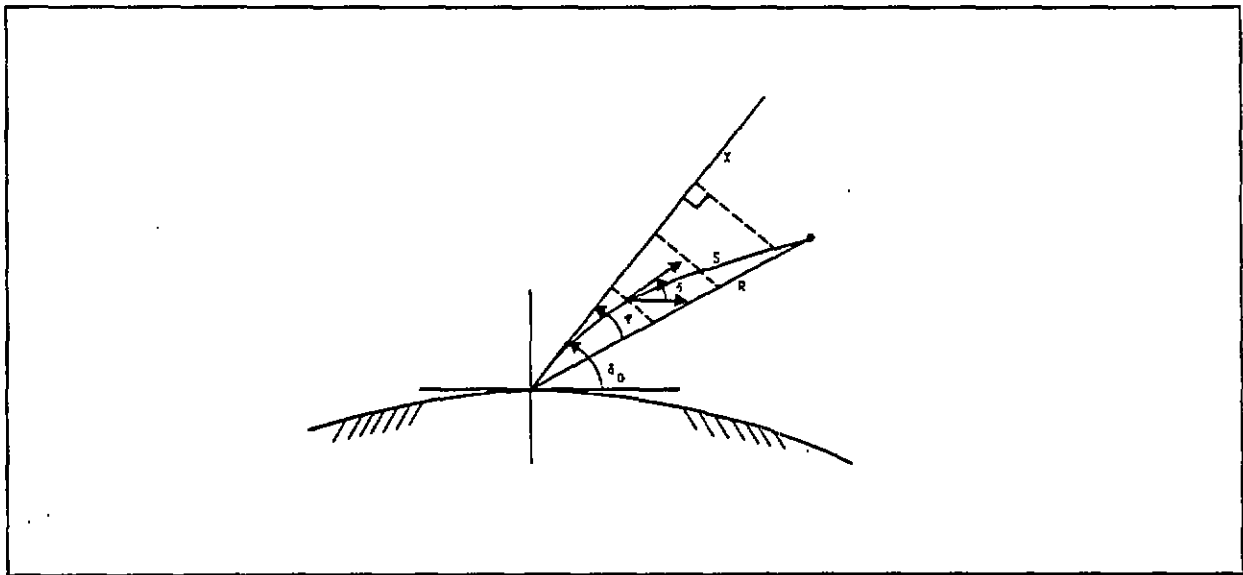


Figure 4-11. Derivation of bending error.

Neither the length nor the direction of R are known a priori to the ray trace. An arbitrary straight line (χ) is defined and the differences in length between the ray and (χ) are accumulated. After the ray trace is complete, the accumulated

differences are then applied as corrections to the ray trace to account for the difference in direction (ψ) between (χ) and line R. With this in mind, the following equation will be used in place of 4-10:

$$\varepsilon_B = S - \chi - (R - \chi) \quad (4-11)$$

where (χ) is assumed the component distance along the straight line defined by the initial direction of the ray. This choice in direction is arbitrary and picked only for convenience.

Differentiating and integrating equation 4-11 with respect to distance gives

$$\varepsilon_B = \int_s \left(1 - \frac{d\chi}{ds} \right) ds - (R - \chi)$$

and since $\frac{d\chi}{ds} = \cos(\delta - \delta_o)$,

$$\varepsilon_B = \int_s [1 - \cos(\delta - \delta_o)] ds - (R - \chi) \quad (4-12)$$

At the completion of the ray trace, the final direction angle ψ can be determined to correct for the bias caused by the arbitrary choice of the χ direction.

Expressing $(R - \chi)$ as $R(1 - \cos\psi)$ and using a trigonometric identity,

$$1 - \cos\psi = 2 \sin^2 \left(\frac{\psi}{2} \right),$$

greater precision is maintained and equation 4-12 becomes

$$\varepsilon_B = \int_s 2 \sin^2 \left[\frac{\delta - \delta_o}{2} \right] ds - R \cdot 2 \sin^2 \left(\frac{\psi}{2} \right) \quad (4-13)$$

The first term in the above equation is solved during the ray trace solution of the differential equations and the last term is a correction applied after the ray trace is complete.

4.2.1.3.2 Range Retardation Correction. The range refraction correction because of retardation (ϵ_R) is defined as the difference between the distance traveled by the ray in a vacuum minus the distance traveled in the atmosphere. The equation is

$$\epsilon_R = \int \left(c - \frac{c}{n} \right) dt$$

Variables can be changed by noting $\frac{ds}{dt} = \frac{c}{n}$ to yield

$$\epsilon_R = \int (n - 1) ds \quad (4-14)$$

4.2.1.3.3 Total Range Correction. The total range refraction correction is the sum of equations 4-14 and 4-15, that is,

$$\epsilon_T = \epsilon_B + \epsilon_R \quad (4-15)$$

and the true range is

$$R_T = R_O - \epsilon_T \quad (4-16)$$

4.2.1.3.4 Elevation Angle Correction. Figure 4-12 shows the relationship which will be used to define the elevation correction.

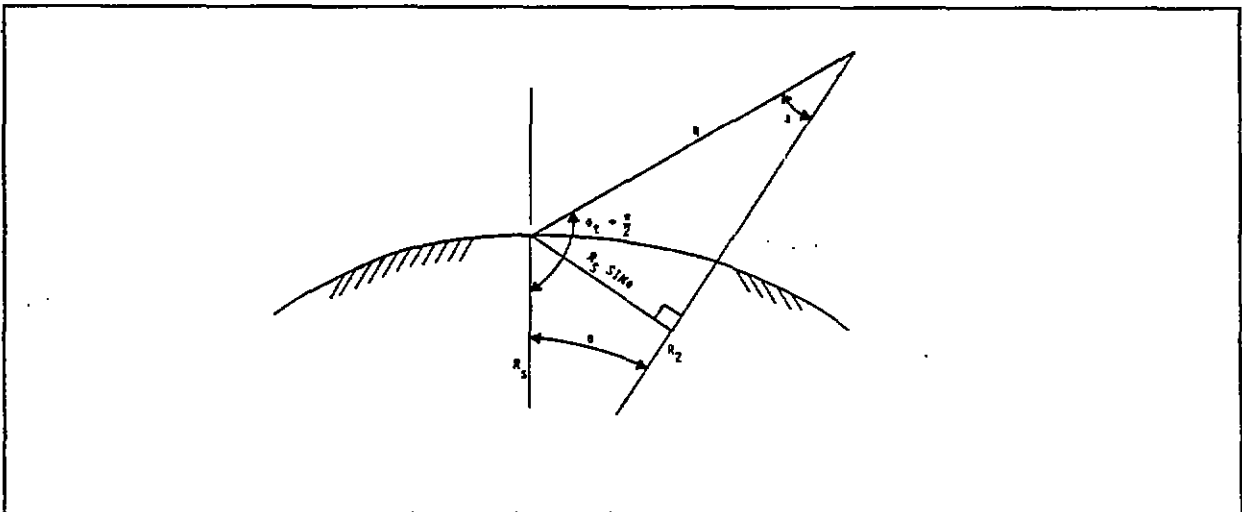


Figure 4-12. Geometry for elevation correction.

From figure 4-12, the law of cosines can be expressed as

$$R_s^2 + 2R_2 \cos(a) = R_2^2 + R^2$$

Solving for $\cos(a)$,

$$\cos(a) = \frac{R_2^2 + R^2 - R_s^2}{2R_2R}$$

Again, using figure 4-12,

$$\sin(a) = \frac{R_s \sin \Theta}{R}$$

so that a , with the proper sign, can be computed as follows

$$a = \tan^{-1} \left(\frac{\sin(a)}{\cos(a)} \right)$$

and the true elevation angle ϕ_t is

$$\phi_t = \frac{\pi}{2} - \Theta - a$$

or

$$\phi_t = \frac{\pi}{2} - \Theta - \tan^{-1} \left[\frac{\left(\frac{R_s \sin \Theta}{R} \right)}{\left(\frac{R_2^2 + R^2 - R_s^2}{2R_2R} \right)} \right]$$

Then, the elevation angle correction is

$$\Delta E = \phi_o - \phi_t$$

4.2.1.4 Solution to the Differential Equations (Ray Trace). The equations to be solved are

$$\frac{d\Theta}{ds} = \frac{\cos\phi}{(R_e+h)} \quad (4-5)$$

$$\frac{dh}{ds} = \sin\phi \quad (4-6)$$

$$\frac{d\delta}{ds} = \frac{1}{n} \cos(\phi) \frac{dn}{dh} \quad (4-9)$$

$$\frac{d\varepsilon_B}{ds} = 2 \sin^2 \left[\frac{\delta - \delta_0}{2} \right] \quad (4-13)$$

$$\frac{d\varepsilon_R}{ds} = n - 1 \quad (4-14)$$

where

$$\phi = \delta + \Theta$$

The differential equations are solved using the Runge-Kutta-Gill numerical method until the input range (S) is satisfied or until vacuum conditions are encountered ($n-1 \leq 10^{-30}$) and no additional profile exists.

4.2.2 Beacon Delay. Beacon delay is a two part error term. The first part is a fixed delay determined by laboratory (or other) means; no derivation is necessary. The second part is simply a statement about the dependency between delay variation and signal strength. No derivation is provided because the functional relationship depends on the characteristics of the individual beacon receiver.

$$\Delta R = \alpha + a_3 \cdot f(S/N)$$

CHAPTER 5

APPLICATION OF ERROR MODEL

The stability and reliability of the coefficients derived by using the error model depend on several factors outside the scope of this material. For completeness, some discussion is warranted at this point. Error coefficients are classified into two separate categories: long term and short term. Long-term coefficients change very slowly, so the measurement frequency is several months. Short-term coefficients can change very rapidly because of mechanical or climatic influences. These measurements should occur more frequently depending on the error type. The error type also determines the method of measurement. Some error terms are best determined using electro-optical equipment, while others are best determined with satellite tracks or some other means. The following table summarizes the methodology used for the FPS-16 radars at the Air Force Flight Test Center and is provided as an example for practical radar calibration.

EXAMPLE OF ERROR MODEL COEFFICIENT COLLECTION METHODOLOGY USED AT AFFTC FOR FPS/16 RADARS			
ERROR TERM	PRIMARY METHOD OF CALIBRATION	SECONDARY METHOD OF CALIBRATION	FREQUENCY OF CALIBRATION
RANGE TERMS			
ZEROSET	A/C CAL SPOT	RANGE REFLECTOR	EVERY MISSION
TIME DELAY	REGRESSED IN BET		EVERY MISSION
VELOCITY SERVO LAG	N/A TYPE 1 SYSTEM	N/A TYPE 1 SYSTEM	N/A
ACCELERATION SERVO LAG	MEASURE KA		SEMI-ANNUAL
BEACON DELAY	A/C CAL SPOT	MEASURED IN LAB.	EVERY MISSION
TRANSIT TIME	PURE MATHEMATICAL	N/A	EVERY MISSION
REFRACTION	RTREF(PMTC)	REEK(ETR)	EVERY MISSION
PULSE WIDTH/BANDWIDTH MISMATCH	A/C CAL SPOT		EVERY MISSION
SURVEY	RE-SURVEY	N/A	AS NEEDED

**EXAMPLE OF ERROR MODEL
COEFFICIENT COLLECTION METHODOLOGY
USED AT AFFTC FOR FPS/16 RADARS**

ERROR TERM	PRIMARY METHOD OF CALIBRATION	SECONDARY METHOD OF CALIBRATION	FREQUENCY OF CALIBRATION
AZIMUTH TERMS			
ZEROSET	STARS	SATELLITE	BI-WEEKLY
TIME DELAY	REGRESSED IN BET		EVERY MISSION
VELOCITY SERVO LAG	N/A TYPE 2 SYSTEM	N/A TYPE 2 SYSTEM	N/A
ACCELERATION SERVO LAG	MEASURE KA		SEMI-ANNUAL
MISLEVEL	TILTMETER/TALYVEL	STARS	EVERY MISSION
WOBBLE	TILTMETER/TALYVEL	STARS	EVERY MISSION
TRANSIT TIME	PURE MATHEMATICAL	N/A	EVERY MISSION
NON-ORTHOGONALITY	E/O CALIBRATIONS		ANNUAL
NON-LINEARITY	E/O CALIBRATIONS		SEMI-ANNUAL
ELECTRICAL MISALIGNMENT	SATELLITE	A/C CALIBRATION	BI-WEEKLY
SURVEY	RE-SURVEY	N/A	AS NEEDED
VERTICAL DEFLECTION	SURVEY	N/A	A NEEDED
ELEVATION TERMS			
ZEROSET	SATELLITE	A/C CALIBRATION	BI-WEEKLY
TIME DELAY	REGRESSED IN BET		EVERY MISSION
VELOCITY SERVO LOG	N/A TYPE 2 SYSTEM	N/A TYPE 2 SYSTEM	N/A
ACCELERATION SERVO LAG	MEASURE KA		SEMI-ANNUAL
MISLEVEL	TILTMETER/TALYVEL	STARS	EVERY MISSION
WOBBLE	TILTMETER/TALYVEL	STARS	EVERY MISSION
TRANSIT TIME	PURE MATHEMATICAL	N/A	EVERY MISSION
NON-LINEARITY	E/O CALIBRATIONS		SEMI-ANNUAL
ANTENNA DROOP	SATELLITE	A/C CALIBRATION	BI-WEEKLY
SURVEY	RE-SURVEY	N/A	AS NEEDED
VERTICAL DEFLECTION	SURVEY	N/A	AS NEEDED
REFRACTION	RTREF(PMTC)	REEK(ETR)	EVERY MISSION

APPENDIX A
RELATED DOCUMENTS

APPENDIX A

RELATED DOCUMENTS

RANGE REFERENCE TABLE

OLD NAME	NEW NAME
EASTERN TEST RANGE	45TH SPACE WING
PACIFIC MISSILE RANGE POINT MUGU	NAVAL AIR WARFARE CENTER WEAPONS DIVISION POINT MUGU
SAMTEC	30TH SPACE WING
WESTERN TEST RANGE	30TH SPACE WING
USAKA	KWAJALEIN MISSILE RANGE

STATIC ERROR

Metric Error Correction Measurements for the MPS-36 Radars at
Kwajalein, RISA-72-002
March 1972 Kwajalein Missile Range

Standard Operating Procedures, SOP 203.206, FPQ-19 Mission
Calibrations
August 1988 Kwajalein Missile Range

Azimuth Encoder Zero Set (Starshot) Error Measurement
Procedure, AN/MPS-25 (2.2.6.1)
January 1971 (Revised February 1973) Pacific Missile Range

Derivation of Systematic Errors for WTR Radar Systems,
 FDEA-66-4
 May 1966 Western Test Range

Radar Data Correction Program, ER-021-85
 May 1985 Air Force Flight Test
 Center

Standard Operating Procedure, SOP 203.020, MPS-36 E/O
 Calibrations Addendum to RISA 72-002
 April 1989 Kwajalein Missile Range

Elevation Encoder Zero Set Error Measurement Procedure
 (1.2.6.2), AN/FPS-16
 June 1972 Pacific Missile Range

Elevation Encoder Zero Set Error Measurement Procedure
 (2.2.6.2), AN/MPS-25
 November 1970 (Revised May 1972) Pacific Missile Range

Azimuth Encoder Zero Reference, MPS-36 Radar-REDS (Section 2.3,
 4.1.4, and 4.2 of RISA 74-008)
 September 1974 Kwajalein Missile Range

Metric Systems Testing Report, 30-70-50, MIPIR Star Shot
 Test - ARCS, Procedure 4.2.2
 August 1971 SAMTEC

Metric Systems Testing Report, 30-70-50, AN/MPS-36 Star Shot
 Test, Procedure 4.3.1
 April 1974 SAMTEC

Elevation Encoder Reference, MPS-36 Radar-REDS (Sections 2.4,
 4.1.4 and 4.2 of RISA 74-008)
 September 1974 Kwajalein Missile Range

AZIMUTH/ELEVATION ENCODER NONLINEARITY

Metric Error Correction Measurements for the MPS-36 Radar at
 Kwajalein, RISA-72-002
 March 1972 Kwajalein Missile Range

Azimuth Encoder Nonlinearity Error Measurement Procedure,
 AN/MPS-25 (2.2.5.1 and 2.2.5.3)
 November 1970 Pacific Missile Range

Standard Operating Procedure, SOP 203.103, MPS-36 Radar Error
 Determination System (REDS) Operation
 May 1989 Kwajalein Missile Range

Standard Operating Procedure, SOP 203.206, FPQ-19 Mission
 Calibrations
 August 1988 Kwajalein Missile Range

Standard Operating Procedure, SOP 203.020, MPS-36 E/O
 Calibrations Addendum to RISA 72-002
 April 1989 Kwajalein Missile Range

Derivation of Systematic Errors for WTR Radar Systems, FDEA-66-4
 May 1966 Western Test Range

Radar Data Correction Program, ER-021-85
 May 1985 Air Force Flight Test
 Center

Elevation Encoder Nonlinearity Error Measurement Procedure,
 AN/FPS-16 (SPIB I.D. No. 1.2.5.2 and 1.2.5.4)
 July 1972 Pacific Missile Range

Elevation Encoder Nonlinearity Error Measurement Procedures,
 AN/MPS-25 (2.2.5.2 and 2.2.5.4)
 November 1970 (Revised May 1972) Pacific Missile Range

Metric Systems Testing Report, 30-70-50, Revision 1, Azimuth
 Encoder Nonlinearity Test, Procedure 2.2.1, FPS-16
 May 1971 SAMTEC

Metric Systems Testing Report, 30-70-50, Azimuth Encoder
 Nonlinearity Test, Procedure 2.2.1, MIPIR
 September 1970 SAMTEC

Metric Systems Testing Report, 30-70-50, Azimuth Encoder
 Nonlinearity Test, Procedure 2.3.1, AN/MPS-36
 February 1973 SAMTEC

Azimuth and Elevation Encoder Linearity, MPS-36 Radar-REDS
 (Section 2.10 and 4.2 of RISA 74-008)
 September 1974 Kwajalein Missile Range

Metric Systems Testing Report, 30-70-50, Revision 1, Elevation
 Encoder Nonlinearity Test, Procedure 2.1.2, FPS-16
 June 1971 SAMTEC

Metric Systems Testing Report, 30-70-50, Elevation Encoder
 Nonlinearity Test, Procedure 2.2.2, MIPIR
 September 1970 SAMTEC

Metric Systems Testing Report, 30-70-50, Elevation Encoder
 Nonlinearity Test, Procedure 2.3.2 AN/MPS-36
 February 1973 SAMTEC

Azimuth and Elevation Encoder Linearity, Radar-REDS (Sections 2.10 and 4.2 of RISA 74-008), MPS-36
September 1974 Kwajalein Missile Range

SERVO LAG

Metric Error Correction Measurement for the MPS-36 Radars at Kwajalein, RISA-72-002
March 1972 Kwajalein Missile Range

Procedure for Field Determination of K_V , K_A
May 1972 Pacific Missile Range

Derivation of Systematic Errors for WTR Radar Systems, FDEA-66-4
May 1966 Western Test Range

Radar Data Correction Program, ER-021-85
May 1985 Air Force Flight Test Center

Metric Systems Testing, 30-70-50, Revision 1, Procedures 3.1.1, K_V , K_A Determination for FPS-16 Radars
June 1972 SAMTEC

Metric Systems Testing Report, 30-70-50, Revision 1, Procedures 3.2.1, K_V , K_A Determination for MIPIR Radars
April 1972 SAMTEC

VERTICAL DEFLECTION

Metric Error Correction Measurements for the MPS-36 Radars at Kwajalein, RISA-72-002
March 1972 Kwajalein Missile Range

DMA Technical Report Geodesy for the Layman, DMA TR 80-003
December 1983 Defense Mapping Agency

J. J. O'Connor, Methods of Trajectory Mechanics, ESMC-TR-80-45
May 1981 Eastern Space and Missile Center

PEDESTAL MISLEVEL AND AZIMUTH ROLLER PATH ERROR

Metric Error Correction Measurements for the MPS-36 Radars at Kwajalein, RISA-72-002
March 1972 Kwajalein Missile Range

Standard Operating Procedures, SOP 203.206, FPQ-19 Mission
Calibrations
August 1988 Kwajalein Missile Range

Standard Operating Procedure, SOP 203.104, AN/MPS-36 Radar
System Computer Program Support Functions
May 1989 Kwajalein Missile Range

Standard Operating Procedure, SOP 203.100, AN/MPS-36 Radar
System Operation and Maintenance
May 1989 Kwajalein Missile Range

Pedestal Mislevel and Azimuth Roller Path Error Measurement
Procedure (using Brunson Electronic Level)
February 1970 Pacific Missile Range

Pedestal Mislevel and Azimuth Bearing Wobble Error Measurement
Procedure Brunson Electronic Level Method (RADEM No. 2.2.2.1,
2.2.2.2., 2.2.2.3)
February 1970 Pacific Missile Range

Derivation of Systematic Errors for WTR Radar Systems, FDEA-66-4
May 1966 Western Test Range

Radar Data Correction Program, ER-021-85
May 1985 Air Force Flight Test
Center

Pedestal Mislevel and Azimuth Bearing Wobble Error Measurement
Procedure, Brunson Electronic Level Method (RADEM No. 2.2.2.1,
2.2.2.2, 2.2.2.3), (AN/MPS-25 Radar Error Measurement
Procedure), Preliminary
February 1970 Pacific Missile Range

Metric Systems Testing Report, 30-70-50, Procedure 2.1.3,
FPS-16
September 1970 SAMTEC

Metric Systems Testing Report, 30-70-50, Procedure 2.2.3, MIPIR
September 1970 SAMTEC

Metric Systems Testing Report, 30-70-50, Procedure 2.3.3,
AN/MPS36
March 1973 SAMTEC

Pedestal Mislevel or Rollerpath Error, MPS-36, REDS (Section
2.2 of RISA 74-008)
September 1974 Kwajalein Missile Range

TRANSIT TIME

Derivation of Systematic Errors for WTR Radar Systems, FDEA-66-4
May 1966 Western Test Range

BEACON DELAY

Derivation of Systematic Errors for WTR Radar Systems, FDEA-66-4
May 1966 Western Test Range

ELECTRICAL MISALIGNMENT

Derivation of Systematic Errors for WTR Radar Systems, FDEA-66-4
May 1966 Western Test Range

Radar Data Correction Program, ER-021-85
May 1985 Air Force Flight Test
Center

Metric Systems Testing Report, 30-70-50, RF Alignment Flight
Test, Procedure 5.1.1, FPS-16
September 1970 SAMTEC

Metric Systems Testing Report, 30-70-50, RF Alignment Flight
Test, Procedure 5.2.1, MIPIR
September 1970 SAMTEC

Metric Systems Testing Report, 30-70-50, RF Alignment Flight
Test, Procedure 12.3, MIPIR-ARCS, Site 023003
November 1970 SAMTEC

Metric Systems Testing Report, 30-70-50, RF Misalignment Flight
Test, Procedure 5.3.1, AN/MPS-36
April 1974 SAMTEC

RF Misalignment Flight Test, FPS-16-ARCS MPL 08884, Rev 2
Date Unknown SAMTEC

Metric Systems Testing Report, 30-70-50, Satellite Test,
Procedure 13.3, MIPIR-ARCS
November 1974 SAMTEC

RF and REDS Collimation Orthogonality Correction, MPS-36 Radar
(Section 2.7, 4.1.4 and 4.2 of RISA 74-008)
September 1974 Kwajalein Missile Range

AZIMUTH/ELEVATION AXIS NONORTHOGONALITY MEASUREMENTS

Metric Error Correction Measurements for the MPS-36 Radars at Kwajalein, RISA-72-002
March 1972 Kwajalein Missile Range

Standard Operating Procedures, SOP 203-206, FPQ-19 Mission Calibrations
August 1988 Kwajalein Missile Range

Standard Operating Procedures, SOP 203-103, MPS-36 Radar Error Determination System (REDS) Operations
May 1989 Kwajalein Missile Range

Elevation to Azimuth Axis Nonorthogonality (Standards) Error Measurement Procedure, AN/MPS-25 (2.2.3.1 and 2.2.3.2)
December 1970 (Revised February 1973) Pacific Missile Range

RF-Axis Nonorthogonality Error Measurement Procedure Autotrack Method (Landbased Mod-1 Mount) (RADEM No. 2.3.3.1 and 2.3.3.3)
November 1970 Pacific Missile Range

RF-Axis Nonorthogonality and RF-Axis Shift Error Measurement Procedure, Antenna Phase Center Method (Landbased MOD-1 Mount) (RADEM No. 2.3.3.1, 2.3.3.3, 2.8.3.1, 2.8.3.3 and 2.8.3.5)
January 1971 Pacific Missile Range

Derivation of Systematic Errors for WTR Radar Systems, FDEA-66-4
May 1966 Western Test Range

Radar Data Correction Program, ER-021-85
May 1985 Air Force Flight Test Center

Metric Systems Testing Report, 30-70-50, Nonorthogonality Test Procedure, Procedure 2.1.4, FPS-16
September 1970 SAMTEC

Metric Systems Testing Report, 30-70-50, Revision 1, Nonorthogonality Test Procedure, Procedure 2.2.4, MIPIR
March 1971 SAMTEC

Metric Systems Testing Report, 30-70-50, Nonorthogonality Test Procedure, Procedure 2.3.4, AN/MPS-36
February 1973 SAMTEC

Azimuth Axis Versus Elevation Orthogonality (Standards), Sections 2.5 and 4.2 of RISA 74-008, MPS-36 Radar-REDS
September 1974 Kwajalein Missile Range

DROOP

Metric Error Correction Measurements for the MPS-36 Radars at Kwajalein, RISA-72-002
March 1972 Kwajalein Missile Range

Standard Operating Procedure, SOP 203.206, FPQ-19 Mission Calibration
August 1988 Kwajalein Missile Range

Standard Operating Procedure, SOP 203.020, MPS-36 E/O Calibrations, Addendum to RISA 72-002
April 1989 Kwajalein Missile Range

Standard Operating Procedure, SOP 203.103, MPS-36 Radar Error Determination System (REDS) Operation
May 1989 Kwajalein Missile Range

Derivation of Systematic Errors for WTR Radar Systems, FDEA-66-4
May 1966 Western Test Range

Radar Data Correction Program, ER-021-85
May 1985 Air Force Flight Test Center

RF and REDS Droop Correction, MPS-36 Radar (Sections 2.8, 4.1.4 and 4.2 of RISA 74-008)
September 1974 Kwajalein Missile Range

K. R. Symon, Mechanics 3rd Edition, Addison-Wesley Publishing Company, 1971

ATMOSPHERIC REFRACTION

Correcting Radar Data for Atmospheric Refraction, No. 3430-7-68
March 1968 Pacific Missile Range

Atmospheric Ray Tracing and Refraction Correction, Technical Publication, TP-82-01
October 1981 Pacific Missile Range

Determination of Elevation and Slant Range Errors Due to Atmospheric Refraction, Technical Note No. 3280-6
December 1962 (Revised 1964) Pacific Missile Range

3423 Working Note 5-73, An Evaluation of Atmospheric Refraction Corrections of Radar Data for OP 3556
Date Unknown Pacific Missile Range

3423 Working Note 6-73, An Evaluation of Atmospheric Refraction Corrections of Radar Data for OP 4565
Date Unknown Pacific Missile Range

Derivation of Systematic Errors for WTR Radar Systems, FDEA-66-4
May 1966 Western Test Range

Radar Data Correction Program, ER-021-85
May 1985 Air Force Flight Test Center

Technical Presentation at Joint Session of Data Reduction and Computing and Electromagnetic Propagation Working Groups of IRIG, EPWG Document 101-58
October 1957 Range Commanders Council

Atmospheric Refraction Correction Program, Tech. Note. No. 3430-35-68
December 1968 Pacific Missile Range

Altitude Error at 50 NMI Due to Refraction, For a Range of Atmospheric Profiles Observed at Point Mugu, Project RIMCOM, Geophysics Division
Date Unknown Pacific Missile Range

An Evaluation of Atmospheric Refraction Correction of Radar Data, Code 3442 Working Notes
Date Unknown Pacific Missile Range

Environmental Measurements at PMR, Ultraviolet and RF Measurements
January 1975 Pacific Missile Range

G. D. Trimble, REEK-REEK: Spherically Stratified & Two Dimensional Profile Refraction Corrections for Range and Elevation (Technical Memorandum 5350-70-4), ETV-70-90
April 1970 Eastern Test Range

OPTICAL SYSTEM ERROR MEASUREMENT

Standard Operating Procedure, SOP 203.103, MPS-36 Radar Error Determination System (REDS) Operation
May 1989 Kwajalein Missile Range

Boresight Telescope Optical Axis Nonsymmetry Error Measurement Procedure (RADEM No. 2.3.5.1 and 2.3.5.2)
December 1970 Pacific Missile Range

Boresight Telescope Optical Calibration Target Nonlevel Error Measurement Procedure (RADEM No. 2.3.5.3)

December 1970	Pacific Missile Range
Metric Systems Testing Report, 30-70-50, Boresight Camera Calibration, Procedure 4.1.1, FPS-16 September 1970	SAMTEC
Metric Systems Testing Report, 30-70-50, Boresight Camera Calibration, Procedure 4.2.1, MIPIR September 1970	SAMTEC
Metric Systems Testing Report, 30-70-50, Star Shot Test, Procedure 4.3.1, AN/MPS-36 April 1974	SAMTEC
Metric Systems Testing Report, 30-70-50, Star Shot Test, Procedure 11-3, MIPIR-ARCS November 1974	SAMTEC
MPS-36 Radar, REDS-Boresight (Section 4.1.4 and 4.1.5 of RISA 74-008) September 1974	Kwajalein Missile Range

MISCELLANEOUS

80 Most Significant Radars Errors, PMR-JRIAIG 20-73 August 1973 (Revised April 1976)	Pacific Missile Range
Estimated Magnitude of 233 AN/FPS-16 Radar Errors, PMR-JRIAIG 1-73 January 1973 (Revised May 1976)	Pacific Missile Range
Position Uncertainty Due to Systematic Errors in Each FPS-16 and MPS-25 Radar Categorized by Task March 1975	Pacific Missile Range
Derivation of Systematic Errors for WTR Radar Systems, FDEA-66-4 May 1966	Western Test Range
Multiple Target Instrumentation Radar Calibration Subsystem Software Specification September 1982	NAWC-WD
AN/MPS-36 Radar Error Determination System (REDS) Category III Performance Evaluation Experiment Requirement, RISA-74-008 September 1974	Kwajalein Missile Range
Calibration Test Procedure for FPS-16, MIPIR, MPS-36, FPQ, SAMTEC SOP 2111.0 - SAMTEC SOP 2112.08 Date Unknown	SAMTEC

MPS-36 Radar Calibrations Procedure December 1988	Utah Test and Training Range
Radar Calibration Procedures June 1991	Air Force Flight Test Center
IRIG Radar Calibration Catalog, IRIG Documents 256-77 and 135-77 July 1977	Range Commanders Council
Error Sources in Precision Trajectory Radar Calibration, IRIG Document 117-69 February 1969	Range Commanders Council
Radar Calibration Survey, Pacific Missile Range 3441 Date Unknown	Pacific Missile Range
Metric Error Correction Model for the Kwajalein AN/MPS-36 and AN/FPQ-19 Radars Date Unknown	Kwajalein Missile Range
Final Report Range Test and Evaluation Program, AN/TPQ-39(V) Digital Instrumentation Radar Date Unknown	Utah Test and Training Range
Ascension FPQ-15 Radar Sensitivity and Coherent Data Recording Improvements February 1991	Range Commanders Council
Range Commanders Council Organization Policy Document November 1990	Range Commanders Council

ENDNOTES

1. Range Commanders Council Organization Policy Document
November 1990 Range Commanders Council
2. IRIG Radar Calibration Catalog, IRIG Documents 256-77
July 1977 Range Commanders Council
3. Derivation of Systematic Errors for WTR Radar Systems,
FDEA-66-4
May 1966 Western Test Range
4. Radar Data Correction Program, ER-021-85
May 1985 Air Force Flight Test
Center
5. Error Sources in Precision Trajectory Radar Calibration,
IRIG Document 117-69
February 1969 Range Commanders Council
6. K. R. Symon, Mechanics 3rd Edition, Addison-Wesley Publishing
Company, 1971
7. J. J. O'Connor, Methods of Trajectory Mechanics,
ESMC-TR-80-45
May 1981 Eastern Space and Missile
Center
8. DMA Technical Report, Geodesy for the Layman, DMA TR 80-003
December 1983 Defense Mapping Agency
9. G. D. Trimble, REEK-REEK: Spherically Stratified & Two
Dimensional Profile Refraction Corrections for Range and
Elevation (Technical Memorandum 5350-70-4), ETV-70-90
April 1970 Eastern Test Range